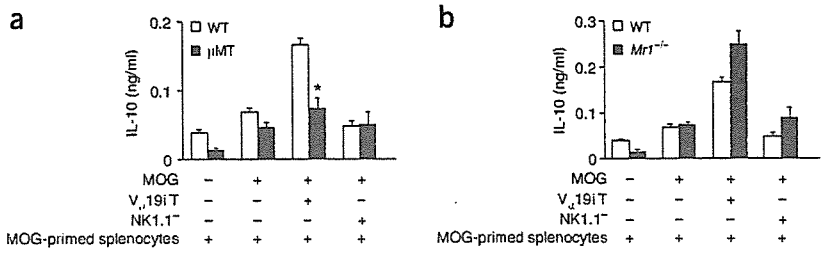

Figure 6 V_α19i T cell–induced IL-10 production is partially B cell dependent but completely MR1 independent. Cytometric bead assay of IL-10 in the supernatants of liver V_α19i T cells from naive V_α19iTg*Cd1d1*$^{-/-}$ mice, cultured for 72 h with MOG(35–55) plus MOG(35–55)-specific splenocytes from wild-type nontransgenic or B cell–deficient μMT mice (a) or from wild-type nontransgenic or MR1-deficient mice (b). Data represent mean ± s.e.m. of duplicate samples from three independent experiments. *, $P < 0.05$, compared with control (two-tailed Student's *t*-test).

CD3$^+$NK1.1$^+$ or CD14$^+$ cells using intracellular cytokine flow cytometry. The addition of V_α19i T cells greatly increased IL-10 production by CD19$^+$ B cells and CD3$^+$ NK1.1$^+$ NKT cells (Fig. 5a). CD4$^+$ and CD8$^+$ T cells also showed slight increases in IL-10 production in the presence of V_α19i T cells. To demonstrate that B cells were the main IL-10 producing cells *in vivo*, we extracted RNA from sorted splenic CD4$^+$ T cells or CD19$^+$ B cells from V_α19iTg*Cd1d1*$^{-/-}$ or nontransgenic mice with EAE (Fig. 5b). In agreement with the results of the *in vitro* coculture system, we found that B cells isolated from V_α19iTg*Cd1d1*$^{-/-}$ mice had higher expression of mRNA transcripts encoding IL-10 than did T cells (Fig. 5b). In addition, B cells from V_α19iTg*Cd1d1*$^{-/-}$ mice had higher expression of *Il10* transcripts than did B cells from *Cd1d1*$^{-/-}$ mice (Fig. 5b). In contrast, CD4$^+$ T cells from V_α19iTg*Cd1d1*$^{-/-}$ mice had lower expression of T_H1 cytokine–encoding mRNA transcripts than did CD4$^+$ T cells from *Cd1d1*$^{-/-}$ mice (Fig. 5b).

To determine if V_α19i T cell–B cell interactions are essential for IL-10 production in the coculture system, we immunized B cell–deficient (μMT) mice with MOG(35–55) to obtain a source of MOG-primed spleen cells lacking B cells. After culture together with V_α19i T cells, B cell–deficient splenocytes produced less IL-10 than did wild-type nontransgenic splenocytes (Fig. 6a). As μMT knockout mice may have unusual follicular architecture, to exclude potential indirect effects we repeated these coculture experiments using B cell–depleted wild-type nontransgenic splenocyte samples. B cell–depleted splenocyte samples produced less IL-10 than did nondepleted splenocyte samples whereas the readdition of wild-type B cells to B cell–depleted splenocyte samples restored IL-10 production (56.3 ± 1.2 pg/ml for B cell–depleted splenocyte samples; 126.0 ± 4.4 pg/ml for B cell–depleted splenocyte samples with B cells 'added back'; and 170.4 ± 0.8 pg/ml for nondepleted splenocyte samples).

We hypothesized that an interaction between MR1 on B cells and the V_α19i TCR on T cells could induce IL-10 secretion from both cell types. To test that, we immunized *Mr1*$^{-/-}$ mice with MOG(35–55), followed by coculture experiments. In the absence of MR1, V_α19i T cell–mediated IL-10 production was not reduced (Fig. 6b). These results suggest that V_α19i T cell–induced IL-10 production can occur at least in part through MR1-independent interaction with B cells. However, non–B cells also seem to contribute to V_α19i T cell–induced IL-10 production.

Costimulation in V_α19i T cell–induced IL-10 production

Naive V_α19i T cells from V_α19iTg*Cd1d1*$^{-/-}$ mice expressed more of the costimulatory molecules CD278 (ICOS), CD86 (B7-2), CD154 (CD40L) and CD28 than did naive splenic T cells (Fig. 7a). V_α19i T cells also expressed CD44 more 'brightly' than did naive T cells (data not shown). These results indicate that V_α19i T cells have an activated or memory phenotype, similar to that of V_α14i NKT cells[1] and 'mucosal-associated invariant T cells' isolated from gut mucosa[2].

Given that MR1 is not required for IL-10 production, we hypothesized that costimulatory interactions may provide the stimulus for IL-10 production. To test that, we repeated the coculture experiments in the presence of blocking antibodies specific for the costimulatory molecules B7RP-1, CD80, CD86 and CD40L. We found that blockade of each costimulatory pathway resulted in significantly lower IL-10 secretion than that of control cocultures treated with control immunoglobulin (Fig. 7b). However, blockade of the ICOS–B7RP-1 pathway inhibited IL-10 production most substantially. To extend those

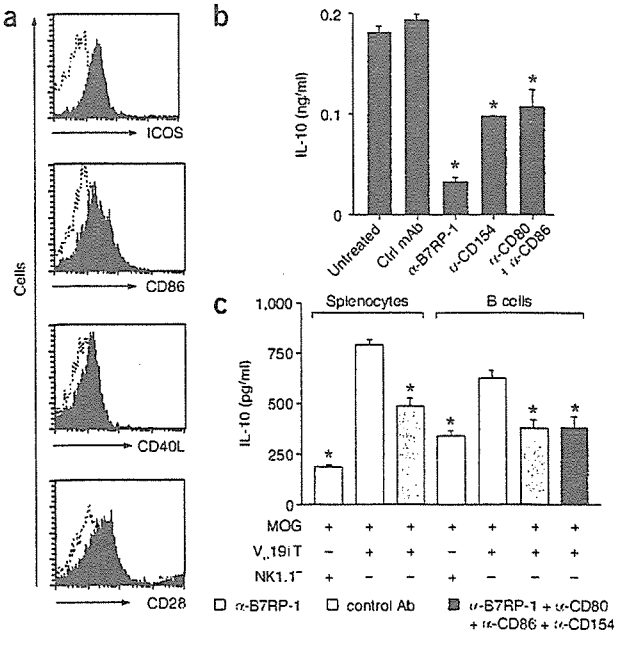

Figure 7 ICOS–B7RP-1 costimulation contributes to V_α19i T cell–induced B cell IL-10 production. (a) Flow cytometry of costimulatory molecule expression on the surface of liver V_α19i T cells (filled histograms) and naive splenic T cells from C57BL/6 mice (dotted lines). Data are representative of three separate experiments. (b) Cytometric bead assay of IL-10 in the supernatants of liver V_α19i T cells from naive mice, cultured with MOG(35–55) and MOG(35–55)-specific splenocytes from wild-type nontransgenic EAE mice in the presence of isotype-matched control antibody (Ctrl mAb) or of blocking antibodies specific to various costimulatory molecules (α–; below graph), measured after 72 h of incubation. Data are representative of two separate experiments. (c) Cytometric bead assay of IL-10 in the supernatants of liver V_α19i T cells from naive V_α19iTg*Cd1d1*$^{-/-}$ mice, cultured with MOG(35–55) and MOG(35–55)-specific splenocytes or sorted B cells from wild-type nontransgenic EAE mice in the presence of various antibodies (key), measured after 72 h of incubation. *, $P < 0.001$, compared with control groups (analysis of variance). Data represent mean ± s.e.m. of triplicate samples from two separate experiments.

findings further, we cultured V_α19i T cells together with purified B cells. This resulted in B7RP-1-dependent IL-10 production (**Fig. 7c**). B7RP-1 blockade partially inhibited IL-10 production in cocultures of V_α19i T cells and splenocytes and fully inhibited IL-10 production in cocultures of V_α19i T cells and purified B cells (**Fig. 7c**). These results suggest that although B cells are a chief producer of IL-10 in this system, other cell types also contribute to V_α19i T cell–induced IL-10 production. Furthermore, the ICOS–B7RP-1 pathway is vital for V_α19i T cell–induced, B cell–mediated IL-10 production, as blockade with a combination of antibodies to costimulatory molecules (B7RP-1, CD80, CD86 and CD40L) inhibited IL-10 to the same degree as anti-B7RP-1 alone (**Fig. 7c**). However, other costimulatory molecules are involved in V_α19i T cell–induced IL-10 production from whole splenocytes (**Fig. 7b**).

DISCUSSION

Although T cells expressing the invariant V_α19-J_α33 TCR chain were first identified in 1993 (ref. 22), knowledge of the immunological function of this invariant T cell population is still limited. Nevertheless, important characteristics of this lymphocyte subset have been characterized, including their restriction by MR1, their TAP (transporter associated with antigen processing)—independent development in rodents, humans and cattle, and the notable interspecies conservation of this invariant TCR. Because CD1d-restricted V_α14i NKT cells, which influence autoimmunity, have similar properties, we speculated that MR1-resricted T cells would also be capable of modifying autoimmunity. However, V_α19i T cells are distinct from V_α14i CD1d-restricted T cells in their 'preferential' distribution in the gut mucosa and their dependence on the presence of B cells and gut flora.

V_α7.2i T cells, the human homolog of V_α19i T cells, are present in lesions of patients with multiple sclerosis[25]. As multiple sclerosis is a demyelinating disease involving autoimmune T cells, B cells, macrophages and various inflammatory mediators, it is possible that MR1-restricted T cells may regulate ongoing disease activity in the CNS. Using an animal model of multiple sclerosis, we examined the effect of overexpression or deletion of MR1-restricted T cells on disease course and severity. Our study suggests that V_α19i T cells can suppress autoimmune inflammation. In addition, we have shown that V_α19i T cells have a memory or activated surface phenotype and are able to produce large amounts of T_H1 and T_H2 cytokines. NK1.1$^+$ T cells from V_α19iTg mice produced more cytokines than did NK1.1$^+$ T cells from V_α19iTg*Cd1d1*$^{-/-}$ mice, indicating a possible interaction between CD1d- and MR1-restricted lymphocytes.

We undertook several approaches to determine whether V_α19i T cells regulate EAE pathogenesis. Overexpression of V_α19i T cells protected mice from clinical EAE. Inhibition of EAE was associated with reduced infiltration and demyelination of the spinal cord as well as a decrease in the production of disease-promoting T_H1 cytokines in the draining lymph nodes and spleen and a reciprocal increase in IL-10, a well established inhibitor of EAE[27–30]. IL-17-secreting cells, which function independently of T_H1 cells, may promote EAE[31]. Here we determined that the inhibitory effect of V_α19i T cells is biased toward prevention of secretion of T_H1 cytokines rather than IL-17.

A potential limitation of TCR-transgenic models is the possible disruption of conventional TCR diversity, which could skew TCR recognition of MOG. However, this is unlikely, as anti-MOG T cell proliferative responses were similar in wild-type nontransgenic and V_α19iTg mice. Furthermore, we adoptively transferred liver V_α19i T cells from naive V_α19iTg*Cd1d1*$^{-/-}$ mice into wild-type nontransgenic mice with EAE, which express natural TCR diversity. In those experiments, V_α19i T cells effectively inhibited EAE, suggesting that V_α19i T cells have a regulatory function during EAE. However, a potential limitation of our model is the difficulty of obtaining pure V_α19i T cell preparations because of the lack of a V_α19 TCR–specific antibody. Therefore, experiments using sorted CD3$^+$ NK1.1$^+$ cells from V_α19iTg*Cd1d1*$^{-/-}$ mice may also contain small numbers of non–V_α14i TCR NK1.1$^+$ T cells of other TCR specificities. To ascertain whether normal numbers of V_α19i T cells in wild-type nontransgenic mice could be involved during EAE, we induced EAE in *Mr1*$^{-/-}$ mice and found that the absence of V_α19i T cells resulted in a more severe clinical disease than that of wild-type nontransgenic mice.

V_α19i T cells most likely exert their main effects in the peripheral lymphoid tissue, as the reduction in proinflammatory cytokines and increase in IL-10 was in the draining lymph nodes and spleen. We also demonstrated that the protective effect of V_α19i T cells was independent of V_α14i NKT cells by using V_α19iTg mice on a CD1d-deficient background. Notably, we found reduced adhesion molecule expression on effector T cells from V_α19iTg*Cd1d1*$^{-/-}$ mice, which correlated with reduced T cell infiltration of the CNS. However, we did note low numbers of V_α19i T cells (CD3$^+$NK1.1$^+$ from V_α19iTg*Cd1d1*$^{-/-}$mice) and B cells in the CNS of mice with EAE, suggesting that V_α19i T cells may also regulate EAE in the CNS.

Coculture experiments suggested that IL-10-producing B cells are involved in the amelioration of EAE in V_α19iTg*Cd1d1*$^{-/-}$ mice. Notably, that finding is consistent with published studies demonstrating that IL-10-producing B cells are involved in spontaneous remission from EAE and could limit clinical disease when adoptively transferred into mice with EAE[32] or a model of collagen-induced arthritis[33]. However, those results do not exclude the possibility that *in vivo*, other cell types are also involved in V_α19i T cell–mediated immune regulation. B cells express MR1 (ref. 34), and V_α19i T cells are MR1 restricted[7], but IL-10 production was unaffected in coculture experiments with lymphocytes from MR1-deficient mice, suggesting that MR1, although necessary for V_α19i T cell selection, is not essential for V_α19i T cell–induced B cell IL-10 production.

T cell activation requires TCR stimulation as well as costimulatory signals. Many costimulatory molecules that regulate cell activation and cytokine secretion have been identified: ICOS and its ligand B7RP-1, CD40-CD40L and CD28-CD80 and CD28-CD86 (refs. 35–38). ICOS costimulation induces IL-10 production as well as help for B cell maturation and CD40L expression[39,40]. The expression of costimulatory molecules on V_α19i T cells was unknown before; we have demonstrated here that V_α19i T cells express ICOS, CD28, CD86 and CD40L. To determine the contribution of each of these costimulatory signaling pathways on the production of IL-10 after V_α19i T cell–B cell interactions, we repeated the coculture experiments using blocking monoclonal antibody to each of the costimulatory pathways. We found that blockade of the ICOS–B7RP-1 pathway inhibited IL-10 production. Furthermore, blockade of the CD40-CD40L, CD28-CD80 or CD28-CD86 pathway also blocked IL-10 production, although not to the extent seen with ICOS blockade.

Commensal flora in the gut are important for the selection of V_α19i T cells[7]. V_α19i T cells may also control gut production of immunoglobulin A from B cells, suggesting involvement of V_α19i T cells in intestinal B cell regulation[7]. Additionally, IL-10 is important for inhibiting excessive inflammation toward gut flora[41], and it has been shown that IL-10 and transforming growth factor-β are involved in immunoglobulin A synthesis and secretion[42]. In the presence of IL-10 and CD40-CD40L signaling, production of immunoglobulin A is increased[43]. Thus, our findings presented here are consistent with the hypothesis that V_α19i T cells are involved in the homeostasis of gut immunity[2,7]. We have shown that V_α19i T cells help B cells produce

IL-10, which in nonpathogenic conditions may inhibit inflammation against gut flora required for $V_\alpha19i$ T cell selection. Therefore, we propose a model of $V_\alpha19i$ T cell–induced protection from EAE whereby $V_\alpha19i$ T cells interact with B cells in lymphoid tissue through ICOS–B7RP-1 and to a lesser degree through other costimulatory pathways to induce IL-10 production, which in turn can inhibit the production of disease-promoting T_H1 cytokines such as IFN-γ and TNF. In conclusion, here we have identified a protective function for invariant $V_\alpha19i$ T cells in autoimmune disease. In contrast to 'conventional' $V_\alpha14i$ NKT cells, more T cells express the $V_\alpha19i$ TCR human homolog $V_\alpha7.2$-$J_\alpha33$ than in mice and therefore these cells may prove to be useful therapeutic targets for the treatment of autoimmune disease.

METHODS

Mice and induction of EAE. C57BL/6 mice (CLEA Laboratory Animal), μMT mice (Jackson Laboratories), $V_\alpha19iTg$ mice[5], $V_\alpha19iTgCd1d1^{-/-}$ mice, $Cd1d1^{-/-}$ mice and $Mr1^{-/-}$ mice[7] were maintained in specific pathogen–free conditions in accordance with institutional guidelines (National Institute of Neuroscience, Tokyo, Japan.). $Mr1^{-/-}$ mice were backcrossed to C57BL/6 mice for ten generations[24]. Mice were injected subcutaneously with 100 μg MOG(35–55) and 1 mg heat-killed *Mycobacterium tuberculosis* H37RA (Difco) emulsified in complete Freund's adjuvant. Pertussis toxin (200 ng in PBS; List Biological Laboratories) was injected intraperitoneally on days 0 and 2 after immunization. EAE clinical symptoms were assigned scores daily as follows: 0, no clinical signs; 1, loss of tail tonicity; 2, impaired righting reflex; 3, partial hindlimb paralysis; 4, total hindlimb paralysis.

Cell sorting and adoptive transfer. For depletion of NK cells, mice were injected intraperitoneally with 100 μg anti-asialo-GM_1 (ref. 44) 48 h before purification of $V_\alpha19i$ T cells. Liver or spleen cells were isolated from mice by Percoll density-gradient centrifugation, and NKT cells, B cells and T cells were purified with the AutoMACS cell purification system (Miltenyi Biotech). NKT cells were isolated using phycoerythrin-conjugated anti-NK1.1 (PK136; BD Pharmingen) and anti-phycoerythrin microbeads (Miltenyi Biotech). The purity of isolated $NK1.1^+$ T cells, assessed by flow cytometry, was more than 90%. In some experiments, single-cell suspensions were incubated with fluorescein isothiocyanate–anti-CD3 (2C11; BD Pharmingen) and phycoerythrin–anti-NK1.1 (PK136, BD Pharmingen) for sorting by flow cytometry. B cells and T cells were isolated from the spleen with anti-CD19 microbeads or the 'pan T cell' kit (Miltenyi Biotech). For adoptive transfer studies, liver $CD3^+NK1.1^+$ $V_\alpha19i$ T cells were sorted from naive $V_\alpha19iTgCd1d1^{-/-}$ mice as described above, and 1×10^6 $V_\alpha19i$ T cells were injected intraperitoneally into naive C57BL/6 recipient mice on the day of immunization with MOG(35–55). Control groups received identical numbers of $CD3^+NK1.1^-$ hepatic cells.

Cell proliferation and cytokine analysis. For *in vitro* stimulation of sorted $V_\alpha19i$ T cells, $CD3^+NK1.1^+$ and $CD3^+NK1.1^-$ cells were suspended in RPMI 1640 medium (Sigma) supplemented with 10% FCS, 2 mM L-glutamine, 100 U/ml of penicillin-streptomycin, 2 mM sodium pyruvate and 50 μM β-mercaptoethanol and were stimulated with immobilized anti-CD3 (5 μg/ml; BD Pharmingen). Cytokines were measured with inflammation cytometric bead assay kits (BD Biosciences) at 24, 48 and 72 h after stimulation with mouse T_H1-T_H2 cytokines. At 10 d after EAE induction without pertussis toxin, myelin-specific T cell responses were measured. Lymphocytes (1×10^6) were cultured with MOG(35–55) (1–100 μM for proliferation studies and 100 μM for cytokine analysis). Cytokines were measured with a cytometric bead assay kit (BD Biosciences) or an IL-17 enzyme-linked immunosorbent assay kit (BD Pharmingen) at 72 h after stimulation. Identical sets of wells were used for proliferation studies. After 72 h, cells were incubated with [^{3}H]thymidine (1 μCi/well) for the final 16 h of culture and incorporation of radioactivity was analyzed with a β-1205 counter (Pharmacia). Proliferation was determined from triplicate wells for each peptide concentration and is expressed as counts per minute.

Surface marker analysis, quantification of CNS leukocytes and histology. The surface phenotype of sorted $V_\alpha19i$ T cells was analyzed by flow cytometry. Nonspecific staining was inhibited by incubation with anti-CD16/32 (BD Pharmingen). Cells were then stained with fluorescence-labeled antibodies specific for CD4, NK1.1, TCRβ, CD3, CD44, CD49d, CD19, CD8, CD14, CD28, CD278, CD86 or CD154 (BD Pharmingen) or CCR1 and CCR2 (Santa Cruz), followed by phycoerythrin-conjugated anti–goat immunoglobulin G (Santa Cruz), and were analyzed with a FACSCalibur (Becton Dickinson). Intracellular cytokines were analyzed by flow cytometry with the BD Cytofix/Cytoperm kit (BD Pharmingen). Staining of paraffin-embedded spinal cords with luxol fast blue and with haematoxylin and eosin was done by SRL. For quantification by flow cytometry, spinal cords were homogenized through 70-μm nylon mesh and by Percoll density-gradient centrifugation to form single-cell suspensions.

RNA extraction and real-time RT-PCR. The SV Total RNA isolation kit (Promega) was used for isolation of total RNA from sorted liver or splenic NKT cells, T cells or B cells according to the manufacturer's instructions. First-strand cDNA was generated with the Advantage-RT kit (Clontech). The Light Cycler-FastStart DNA Master SYBR Green I kit (Roche Diagnostics) was used for real-time PCR. Gene expression values were normalized to expression of the hypoxanthine guanine phosphoribosyl transferase (*Hprt1*) 'housekeeping' gene. Primers from Bex Co are listed in Supplementary Table 1 online.

Mixed-lymphocyte experiments. MOG(35–55)-specific spleen cells (2×10^6) isolated from wild-type nontransgenic mice 10 d after EAE induction were mixed with liver $V_\alpha19i$ T cells (5×10^5) sorted from naive $V_\alpha19iTgCd1d1^{-/-}$ mice, in the presence of 100 μg/ml of MOG(35–55) in 24-well plates or transwell plates (Corning). Where indicated, MOG(35–55)-specific spleen cells were isolated from $Mr1^{-/-}$ or μMT mice or were subjected to depletion with anti-CD19 microbeads (Miltenyi Biotech). Costimulatory molecules were blocked with 10 μg/ml of anti-B7RP-1 (HK5.3) or anti-CD40L (MR1) or with anti-CD80 and anti-CD86 (16-10A1 and GL1, respectively; all from BD Pharmingen)[35]. After 72 h, cytokines in the supernatant were analyzed by cytometric bead assay, enzyme-linked immunosorbent assay or intracellular flow cytometry. Proliferation of MOG(35–55)-specific lymph node cells was assessed 24 h after the addition of [^{3}H]thymidine (1 μCi/well) to 96-well plates.

Statistics. EAE clinical scores for groups of mice are presented as the mean group clinical score ± s.e.m., and statistical differences were analyzed by the Mann-Whitney U nonparametric ranking test. Cytokine secretion data were analyzed with the two-tailed Student's *t*-test or one-way analysis of variance with Tukey post-analysis for multiple group analysis.

Note: Supplementary information is available on the Nature Immunology website.

ACKNOWLEDGMENTS

We thank S. Gilfillan (Department of Pathology and Immunology, Washington University School of Medicine, St. Louis, Missouri) for $Mr1^{-/-}$ mice. Supported by the Japan Society for the Promotion of Science (P03581 to J.L.C), the Ministry of Health, Labour and Welfare of Japan (T.Y. and S.M.), The Program for Promotion of Fundamental Studies in Health Sciences of the National Institute of Biomedical Innovation (02-5 to T.Y.), Grant-in-Aid for Science Research on Priority Area from Ministry of Education, Science, Sports and Culture of Japan (17047051 to S.M.) and Grant-in-Aid for Scientific Research (B) (18390295 to S.M.) from the Japan Society for the Promotion of Science.

COMPETING INTERESTS STATEMENT

The authors declare that they have no competing financial interests.

Published online at http://www.nature.com/natureimmunology/
Reprints and permissions information is available online at http://npg.nature.com/reprintsandpermissions/

1. Kronenberg, M. Toward an understanding of NKT cell biology: progress and paradox. *Annu. Rev. Immunol.* **23**, 877–900 (2005).
2. Treiner, E. *et al.* Mucosal-associated invariant T (MAIT) cells: an evolutionarily conserved T cell subset. *Microbes Infect.* **7**, 552–559 (2005).
3. Kawano, T. *et al.* CD1d-restricted and TCR-mediated activation of Vα14 NKT cells by glycosylceramides. *Science* **278**, 1626–1629 (1997).

4. Zhou, D. *et al.* Lysosomal glycosphingolipid recognition by NKT cells. *Science* **306**, 1786–1789 (2004).
5. Okamoto, N. *et al.* Synthetic α-mannosyl ceramide as a potent stimulant for an NKT cell repertoire bearing the invariant $V_{\gamma}19$-$J_{\gamma}26$ TCR α chain. *Chem. Biol.* **12**, 677–683 (2005).
6. Chen, Y.H., Chiu, N.M., Mandal, M., Wang, N. & Wang, C.R. Impaired NK1$^+$ T cell development and early IL-4 production in CD1-deficient mice. *Immunity* **6**, 459–467 (1997).
7. Treiner, E. *et al.* Selection of evolutionarily conserved mucosal-associated invariant T cells by MR1. *Nature* **422**, 164–169 (2003).
8. Spada, F.M., Koezuka, Y. & Porcelli, S.A. CD1d-restricted recognition of synthetic glycolipid antigens by human natural killer T cells. *J. Exp. Med.* **188**, 1529–1534 (1998).
9. Tilloy, F. *et al.* An invariant T cell receptor α chain defines a novel TAP-independent major histocompatibility complex class Ib-restricted α/β T cell subpopulation in mammals. *J. Exp. Med.* **189**, 1907–1921 (1999).
10. Godfrey, D.I., MacDonald, H.R., Kronenberg, M., Smyth, M.J. & Van Kaer, L. NKT cells: what's in a name? *Nat. Rev. Immunol.* **4**, 231–237 (2004).
11. Lehuen, A. *et al.* Overexpression of natural killer T cells protects Vα14-Jα281 transgenic nonobese diabetic mice against diabetes. *J. Exp. Med.* **188**, 1831–1839 (1998).
12. Mars, L.T. *et al.* Vα14-Jα281 NKT cells naturally regulate experimental autoimmune encephalomyelitis in nonobese diabetic mice. *J. Immunol.* **168**, 6007–6011 (2002).
13. Wagner, M.J., Hussain, S., Mehan, M., Verdi, J.M. & Delovtch, T.L. A defect in lineage fate decision during fetal thymic invariant NKT cell development may regulate susceptibility to type 1 diabetes. *J. Immunol.* **174**, 6764–6771 (2005).
14. Pál, E. *et al.* Costimulation-dependent modulation of experimental autoimmune encephalomyelitis by ligand stimulation of Vα14 NK T cells. *J. Immunol.* **166**, 662–668 (2001).
15. Sharif, S. *et al.* Activation of natural killer T cells by α-galactosylceramide treatment prevents the onset and recurrence of autoimmune type 1 diabetes. *Nat. Med.* **7**, 1057–1062 (2001).
16. Hong, S. *et al.* The natural killer T-cell ligand α-galactosylceramide prevents autoimmune diabetes in non-obese diabetic mice. *Nat. Med.* **7**, 1052–1056 (2001).
17. Miyamoto, K., Miyake, S. & Yamamura, T. A synthetic glycolipid prevents autoimmune encephalomyelitis by inducing T_H2 bias of natural killer T cells. *Nature* **413**, 531–534 (2001).
18. Chiba, A. *et al.* Suppression of collagen-induced arthritis by natural killer T cell activation with OCH, a sphingosine-truncated analog of α-galactosylceramide. *Arthritis Rheum.* **50**, 305–313 (2004).
19. Miyake, S. & Yamamura, T. Therapeutic potential of glycolipid ligands for natural killer (NK) T cells in the suppression of autoimmune diseases. *Curr. Drug Targets Immune Endocr. Metabol. Disord.* **5**, 315–322 (2005).
20. Chiba, A., Kaieda, S., Oki, S., Yamamura, T. & Miyake, S. The involvement of Vα14 natural killer T cells in the pathogenesis of arthritis in murine models. *Arthritis Rheum.* **52**, 1941–1948 (2005).
21. Kim, H.Y. *et al.* NKT cells promote antibody-induced joint inflammation by suppressing transforming growth factor β1 production. *J. Exp. Med.* **201**, 41–47 (2005).
22. Porcelli, S., Yockey, C.E., Brenner, M.B. & Balk, S.P. Analysis of T cell antigen receptor (TCR) expression by human peripheral blood CD4$^-$8$^-$ α/β T cells demonstrates preferential use of several V_{β} genes and an invariant TCR α chain. *J. Exp. Med.* **178**, 1–16 (1993).
23. Shimamura, M. & Huang, Y.Y. Presence of a novel subset of NKT cells bearing an invariant Vα19.1-Jα26 TCR α chain. *FEBS Lett.* **516**, 97–100 (2002).
24. Kawachi, I., Maldonado, J., Strader, C. & Gilfillan, S. MR1-restricted Vα19i mucosal-associated invariant T cells are innate T cells in the gut lamina propria that provide a rapid and diverse cytokine response. *J. Immunol.* **176**, 1618–1627 (2006).
25. Illés, Z., Shimamura, M., Newcombe, J., Oka, N. & Yamamura, T. Accumulation of Vα7.2-Jα33 invariant T cells in human autoimmune inflammatory lesions in the nervous system. *Int. Immunol.* **16**, 223–230 (2004).
26. Illés, Z. *et al.* Differential expression of NK T cell Vα24JαQ invariant TCR chain in the lesions of multiple sclerosis and chronic inflammatory demyelinating polyneuropathy. *J. Immunol.* **164**, 4375–4381 (2000).
27. Croxford, J.L., Feldmann, M., Chernajovsky, Y. & Baker, D. Different therapeutic outcomes in experimental allergic encephalomyelitis dependent upon the mode of delivery of IL-10: a comparison of the effects of protein, adenoviral or retroviral IL-10 delivery into the central nervous system. *J. Immunol.* **166**, 4124–4130 (2001).
28. Croxford, J.L. *et al.* Cytokine gene therapy in experimental allergic encephalomyelitis by injection of plasmid DNA-cationic liposome complex into the central nervous system. *J. Immunol.* **160**, 5181–5187 (1998).
29. Cua, D.J., Groux, H., Hinton, D.R., Stohlman, S.A. & Coffman, R.L. Transgenic interleukin 10 prevents induction of experimental autoimmune encephalomyelitis. *J. Exp. Med.* **189**, 1005–1010 (1999).
30. Bettelli, E., Nicholson, L.B. & Kuchroo, V.K. IL-10, a key effector regulatory cytokine in experimental autoimmune encephalomyelitis. *J. Autoimmun.* **20**, 265–267 (2003).
31. Langrish, C.L. *et al.* IL-23 drives a pathogenic T cell population that induces autoimmune inflammation. *J. Exp. Med.* **201**, 233–240 (2005).
32. Fillatreau, S., Sweenie, C.H., McGeachy, M.J., Gray, D. & Anderton, S.M. B cells regulate autoimmunity by provision of IL-10. *Nat. Immunol.* **3**, 944–950 (2002).
33. Mauri, C., Gray, D., Mushtaq, N. & Londei, M. Prevention of arthritis by interleukin 10-producing B cells. *J. Exp. Med.* **197**, 489–501 (2003).
34. Riegert, P., Wanner, V. & Bahram, S. Genomics, isoforms, expression, and phylogeny of the MHC class I-related MR1 gene. *J. Immunol.* **161**, 4066–4077 (1998).
35. Hayakawa, Y. *et al.* Differential regulation of Th1 and Th2 functions of NKT cells by CD28 and CD40 costimulatory pathways. *J. Immunol.* **166**, 6012–6018 (2001).
36. Ikarashi, Y. *et al.* Dendritic cell maturation overrules H-2D-mediated natural killer T (NKT) cell inhibition: critical role for B7 in CD1d-dependent NKT cell interferon γ production. *J. Exp. Med.* **194**, 1179–1186 (2001).
37. Kitamura, H. *et al.* The natural killer T (NKT) cell ligand α-galactosylceramide demonstrates its immunopotentiating effect by inducing interleukin (IL)-12 production by dendritic cells and IL-12 receptor expression on NKT cells. *J. Exp. Med.* **189**, 1121–1128 (1999).
38. Kaneda, H. *et al.* ICOS costimulates invariant NKT cell activation. *Biochem. Biophys. Res. Commun.* **327**, 201–207 (2005).
39. Hutloff, A. *et al.* ICOS is an inducible T-cell co-stimulator structurally and functionally related to CD28. *Nature* **397**, 263–266 (1999).
40. McAdam, A.J. *et al.* ICOS is critical for CD40-mediated antibody class switching. *Nature* **409**, 102–105 (2001).
41. Song, F. *et al.* Expression of the neutrophil chemokine KC in the colon of mice with enterocolitis and by intestinal epithelial cell lines: effects of flora and proinflammatory cytokines. *J. Immunol.* **162**, 2275–2280 (1999).
42. Kaneko, M., Akiyama, Y., Takimoto, H. & Kumazawa, Y. Mechanism of up-regulation of immunoglobulin A production in the intestine of mice unresponsive to lipopolysaccharide. *Immunology* **116**, 64–70 (2005).
43. Cognasse, F. *et al.* Differential downstream effects of CD40 ligation mediated by membrane or soluble CD40L and agonistic Ab: a study on purified human B cells. *Int. J. Immunopathol. Pharmacol.* **18**, 65–74 (2005).
44. Muhlen, K.A. *et al.* NK cells, but not NKT cells, are involved in *Pseudomonas aeruginosa* exotoxin A-induced hepatotoxicity in mice. *J. Immunol.* **172**, 3034–3041 (2004).

Differential Expression of CD11c by Peripheral Blood NK Cells Reflects Temporal Activity of Multiple Sclerosis[1]

Toshimasa Aranami, Sachiko Miyake, and Takashi Yamamura[2]

Multiple sclerosis (MS) is an autoimmune disease, showing a great degree of variance in temporal disease activity. We have recently demonstrated that peripheral blood NK cells biased for secreting IL-5 (NK2 bias) are associated with the remission state of MS. In this study, we report that MS patients in remission differentially express CD11c on NK cell surface (operationally defined as $CD11c^{high}$ or $CD11c^{low}$). When we compared $CD11c^{high}$ or $CD11c^{low}$ patients, the expression of IL-5 and GATA-3 in NK cells supposed to endow a disease-protective NK2 phenotype was observed in $CD11c^{low}$ but not in $CD11c^{high}$ patients. In contrast, the $CD11c^{high}$ group showed a higher expression of HLA-DR on NK cells. In vitro studies demonstrated that NK cell stimulatory cytokines such as IL-15 would up-regulate CD11c expression on NK cells. Given previous evidence showing an association between an increased level of proinflammatory cytokines and temporal disease activity in MS, we postulate that inflammatory signals may play a role in inducing the $CD11c^{high}$ NK cell phenotype. Follow-up of a new cohort of patients showed that 6 of 10 $CD11c^{high}$ MS patients developed a clinical relapse within 120 days after evaluation, whereas only 2 of 13 $CD11c^{low}$ developed exacerbated disease ($p = 0.003$). As such, a higher expression of CD11c on NK cells may reflect the temporal activity of MS as well as a loss of regulatory NK2 phenotype, which may allow us to use it as a potential biomarker to monitor the immunological status of MS patients. *The Journal of Immunology,* **2006, 177: 5659–5667.**

Multiple sclerosis (MS)[3] is a chronic inflammatory disease of the CNS, in which autoreactive T cells targeting CNS Ags are presumed to play a pathogenic role (1). A large majority of the patients with MS (~70%), known as relapsing-remitting MS, would develop acute exacerbations of disease between intervals of remission. It is currently believed that relapses are caused by T cell- and Ab-mediated inflammatory reactions to the self-CNS components, and could be controlled at least to some degree by anti-inflammatory therapeutics, immunosuppressants, or plasma exchange.

The clinical course of MS varies greatly among individuals, implicating difficulties to predict the future of each patient. For example, patients who had been clinically inactive in the early stage of illness could abruptly change into active MS accompanying frequent relapses and progressive worsening of neurological conditions. There are a number of unpredictable matters in MS, including an interval between relapses, responsiveness to remedy and the prognosis in terms of neurological disability. To provide better quality of management of the patients, searches of appropriate biomarkers are currently being warranted (2).

We have recently shown that surface phenotype and cytokine secretion pattern of peripheral blood NK cells may reflect the disease activity of MS (3, 4). A combination of quantitative PCR and flow cytometry analysis has revealed that NK cells in clinical remission of MS are characterized by a higher frequency of $CD95^-$ cells as well as a higher expression level of IL-5 than those of healthy subjects (HS) (3). As IL-5-producing NK cells, referred to as NK2 cells (5), could prohibit Th1 cell activation in vitro (3), we interpreted that the NK2 bias in MS may contribute to maintaining the remission state of MS. More recently, we have found that MS patients in remission can be further divided into $CD95^{high}$ and $CD95^{low}$, according to the frequency of $CD95^-$ cells among NK cells (4). Notably, memory T cells reactive to myelin basic protein, a major target Ag in MS, were increased in $CD95^{high}$ patients, compared with $CD95^{low}$. Of note, $CD95^{high}$ NK cells exhibited an ability to actively suppress the autoimmune T cells, whereas those from $CD95^{low}$ patients did not. These results suggest that NK cells may accommodate their function and phenotype to properly counterregulate autoimmune T cells in the remission state of MS.

Recently, a distinct population of NK cells that express CD11c, a prototypical dendritic cell (DC) marker, was identified in mice (6, 7). As the $CD11c^+$ NK cells exhibited both NK and DC functions, they are called as "bitypic NK/DC cells." CD11c associates with integrin CD18 to form CD11c/CD18 complex and is expressed on monocytes, granulocytes, DCs, and a subset of NK cells. Although precise functions are unclear, it has been reported that CD11c is involved in binding of iC3b (8), adhesion to stimulated endothelium (9) or phagocytosis of apoptotic cells (10). The initial purpose of this study was to evaluate CD11c expression and function of $CD11c^+$ NK cells in MS in the line of our research to characterize NK cells in MS. On initiating study, we noticed that there was no significant difference between MS and HS in the frequency of $CD11c^+$ NK cells. However, expression levels of CD11c were significantly higher in MS. We further noticed that up-regulation of CD11c is seen in some, but not all, patients with MS. So we have operationally classified MS into $CD11c^{low}$ and $CD11c^{high}$.

In this study, we demonstrate that IL-5, characteristic of NK2 cells (5), were significantly down-regulated in $CD11c^{high}$ than

Department of Immunology, National Institute of Neuroscience, National Center of Neurology and Psychiatry, Tokyo, Japan

Received for publication May 3, 2006. Accepted for publication July 28, 2006.

The costs of publication of this article were defrayed in part by the payment of page charges. This article must therefore be hereby marked *advertisement* in accordance with 18 U.S.C. Section 1734 solely to indicate this fact.

[1] This work was supported by grants from the Ministry of Health, Labor and Welfare of Japan and the Program for Promotion of Fundamental Studies in Health Sciences of the National Institute of Biomedical Innovation.

[2] Address correspondence and reprint requests to Dr. Takashi Yamamura, Department of Immunology, National Institute of Neuroscience, National Center of Neurology and Psychiatry, 4-1-1 Ogawahigashi, Kodaira, Tokyo 187-8502, Japan. E-mail address: yamamura@ncnp.go.jp

[3] Abbreviations used in this paper: MS, multiple sclerosis; HS, healthy subject; DC, dendritic cell; MFI, mean fluorescence intensity; ECD, energy-coupled dye.

0022-1767/06/$02.00

$CD11c^{low}$ NK cells. In contrast, expression of HLA-DR class II molecule was up-regulated in $CD11c^{high}$ NK cells. Notably, both CD11c and HLA-DR on NK cells were reproducibly induced in vitro in the presence of IL-15 (11) or combination of inflammatory cytokines, known to be increased in the blood of MS (12–14). Furthermore, we found that the remission state of $CD11c^{high}$ is unstable in comparison to $CD11c^{low}$, as judged by an increased number of the patients who exacerbated during the 120 days after examining NK cell phenotypes. These results suggest that the $CD11c^{high}$ group of patients may be in more unstable condition than $CD11c^{low}$, presenting with reduced regulatory functions of NK cells.

Materials and Methods

Subjects

Twenty-five patients with relapsing-remitting MS (15) (male (M)/female (F) = 8/17; age = 37.7 ± 11.1 (year old)) and 10 sex- and age-matched HS (M/F = 3/7; age = 39.9 ± 12.2 (year old)) were enrolled for studying NK cell phenotypes. All the patients were in the state of remission at examination as judged by magnetic resonance imaging scanning and clinical assessment. They had not been given immunosuppressive medications, or corticosteroid for at least 1 mo before examination. They had relatively mild neurological disability (expanded disability status scale ≤4) and could walk to the hospital without any assistance during remission. The same neurologist followed up the patients regularly (every 3–4 wk) and judged the occurrence of relapse by using magnetic resonance imaging and clinical examinations. Information on NK cell phenotype or other immunological parameters was never given to either the neurologist or the patients at the time of evaluation. To precisely determine the onset of relapse, patients were allowed to take examination within a few days after a new symptom appeared. Written informed consent was obtained from all the patients and the Ethics Committee of the National Center of Neuroscience (NCNP) approved the study.

Reagents

Mouse IgG1 isotype control-PE, anti-CD3-energy-coupled dye (ECD), anti-CD4-PE, anti-CD8-PC5, anti-CD56-PC5, anti-CD69-PE, and anti-HLA-DR-FITC mAbs were purchased from Immunotech. Anti-CD11c-PE and anti-CD95-FITC were purchased from BD Pharmingen. Recombinant human cytokines were purchased from PeproTech. AIM-V (Invitrogen Life Technologies) was used for cell culture after supplementing 2 mM L-glutamine, 100 U/ml penicillin, and 100 mg/ml streptomycin (Invitrogen Life Technologies).

Cell preparation and NK cell purification

PBMC were separated by density gradient centrifugation with Ficoll-Hypaque PLUS (Amersham Biosciences). To purify NK cells, PBMC were treated with NK isolation kit II (Miltenyi Biotec) twice, according to the manufacturer's protocol. Briefly, PBMC were labeled with a mixture of biotin-conjugated mAbs reactive to non-NK cells and magnetic microbead-conjugated anti-biotin mAbs. The magnetically labeled non-NK cells were depleted with auto-MACS (Miltenyi Biotec) and this procedure always yielded >95% purity of NK cells when assessed by the proportions of $CD3^-CD56^+$ cells with flow cytometry.

Flow cytometry

To evaluate the expression of CD11c, CD95, or other surface molecules on NK cells, PBMC were stained with anti-CD3-ECD, anti-CD56-PC5, and FITC- or PE-conjugated mAbs against molecules of our interest and were analyzed with EPICS flow cytometry (Beckman Coulter). Mean fluorescence intensity (MFI) of CD11c was measured on gated $CD11c^+$ fraction or whole NK cells.

Stimulation of purified NK cells with proinflammatory cytokines

Purified NK cells (1×10^5/well) were stimulated in the presence or absence of IL-4, IL-8, IL-12, IL-15, IL-18, IL-23, TNF-α, and GM-CSF or combination of IL-12, IL-15, and IL-18 for 3 days. We analyzed CD11c expression after staining the cells with anti-CD11c-PE, anti-CD3-ECD, and anti-CD56-PC5. The concentration of IL-12 was at 10 ng/ml, and those of the other cytokines were at 100 ng/ml.

RT-PCR

Total RNA were extracted with a RNeasy Mini kit (Qiagen) from purified NK cells, and the cDNA were synthesized with Super Script III first strand systems (Invitrogen Life Technologies) according to the manufacturer's protocol. For quantitative analysis of IL-5, IFN-γ, GATA-3, and T-bet, the LightCycler quantitative PCR system (Roche Diagnostics) was used. Relative quantities of mRNA were evaluated after normalizing each expression levels with β-actin expression. PCR primers used were as follows: β-actin-sense, AGAGATGGCCACGGCTGCTT, and -antisense, ATTTGCGGTGGACGATGGAG; IFN-γ-sense, CAGGTCATTCAGATGTAGCG, and -antisense, GCTTTTCGAAGTCATCTCG; IL-5-sense, GCACACTGGAGAGTCAAACT, and -antisense, CACTCGGTGTTCATTACACC; GATA-3-sense, CTACGGAAACTCGGTCAGG, and -antisense, CTGGTACTTGAGGCACTCTT; T-bet-sense, GGAGGACACCGACTAATTTGGGA, and -antisense, AAGCAAGACGCAGCACCAGGTAA.

Statistical analysis of remission rate

We set the first episode of relapse after blood sampling as an end point, although we followed clinical course of each patient for up to 120 days, regardless of whether they developed relapses. No patients developed second relapse during the 120 days. When the neurologist prescribed corticosteroids without knowing any information on the NK cell phenotype, the patient was considered as the dropout at that time point. Remission rate was calculated as Kaplan-Meier survival rate, and statistical difference between $CD11c^{low}$ and $CD11c^{high}$ MS was evaluated with the log-rank test.

Results

CD11c on NK cells is up-regulated in MS remission

First, we confirmed that PBMC from healthy individuals and MS contain $CD11c^+$ NK cells (Fig. 1), which constitute a major population of whole NK cells. We then noticed that proportion of $CD11c^+$ NK cells as well as its levels of expression greatly varied among individuals, particularly in MS. To examine this issue further, we systemically examined 25 MS patients in remission and 10 HS for NK cell expression of CD11c. Whereas 20–80% of NK cells are $CD11c^+$ in HS (Fig. 1*c*), almost all NK cells were $CD11c^+$ in some MS patients (Fig. 1, *c* and *e*). However, reflecting a great degree of variance, comparison between HS and MS did not reveal a significant difference (Fig. 1*c*). In contrast, when we measured the MFI of CD11c expression on $CD11c^+$ NK cells, it was significantly higher in MS as compared with HS (Fig. 1*a*). This difference was also noticed when MFI of CD11c was measured for all the NK cell populations (Fig. 1*b*). It was interesting to know whether the levels of CD11c expression may correlate with NK cell functions. Therefore, we operationally divided the MS patients into $CD11c^{low}$ and $CD11c^{high}$ subgroups (Fig. 1*a*), by setting the border as (the average + 2 × SD) of the values for HS.

$CD11c^{high}$ NK cells express HLA-DR more brightly than $CD11c^{low}$ NK cells

It was previously reported that infection with certain viruses would accompany up-regulation of CD11c on NK cells (16). This raises a possibility that the increased expression of CD11c in $CD11c^{high}$ MS may reflect an activation state of NK cells caused by some sort of stimuli. To verify this hypothesis, we examined surface expression of cell activation markers (CD69 and HLA-DR). Although CD69, an early activation marker, was not detectable on NK cells (Fig. 2*a*), NK cells from MS, particularly $CD11c^{high}$ MS, significantly overexpressed HLA-DR on surface (Fig. 2). Interestingly, HLA-DR expression was also up-regulated on $CD4^+$ T cells from $CD11c^{high}$ MS compared with those from HS (data not shown). These results indicate that NK cells and T cells are differentially activated in $CD11c^{high}$ MS, $CD11c^{low}$ MS, and HS.

Absence of NK2 bias in $CD11c^{high}$ MS

We have previously reported that a higher level of IL-5 expression (NK2 bias) is one of the characteristics of NK cells of MS in

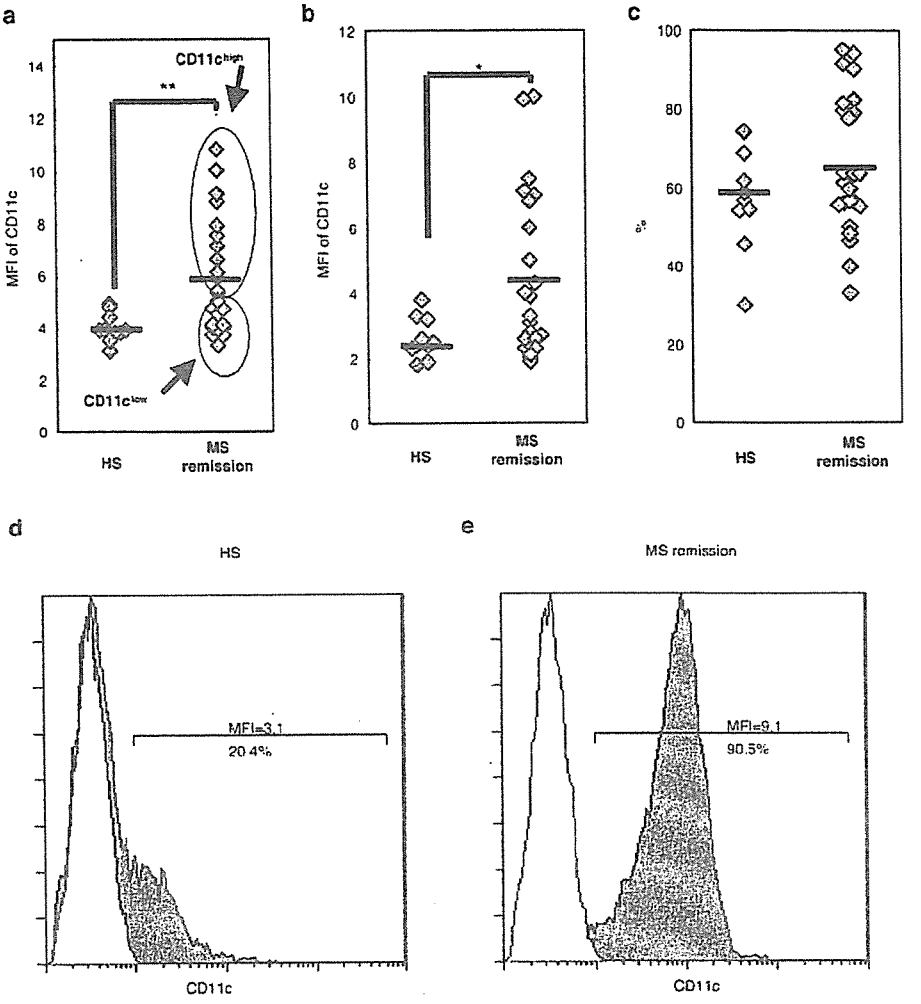

FIGURE 1. CD11c on NK cells is up-regulated in MS in remission. *a*, PBMC from HS (n = 10) and MS patients in remission (n = 25) were stained with anti-CD11c-PE, -CD3-ECD, and -CD56-PC5 mAb, and CD11c expression was measured on the $CD11c^+$ fraction gated within whole NK cells ($CD11c^+CD3^-CD56^+$ cells) as mean fluorescence intensity (MFI). Each dot represents the data from individual patients. $CD11c^{high}$ and $CD11c^{low}$ groups of patients are encircled as described in the text. *b*, In parallel, CD11c expression (MFI) was measured for the whole NK cells ($CD3^-CD56^+$ cells), which yielded a similar result. *c*, The proportions of $CD11c^-$ cells among whole NK cells are plotted. No significant difference was noted between HS and MS remission. *d* and *e*, Representative histogram patterns of CD11c on NK cells (closed histogram) from a single healthy subject (HS) (*d*) and a patient corresponding to $CD11c^{high}$ MS (*e*). Open histograms represent isotype control staining. Values represent proportions of $CD11c^-$ fraction (%) and MFI for $CD11c^-$ cells. Mann-Whitney U test was used for statistical analysis. Horizontal bars indicate the mean values. *, $p < 0.05$; **, $p < 0.01$.

remission (3). Although the mechanism for NK2 bias in MS remains to be further studied, up-regulation of GATA-3 has recently been reported in the induction of NK2 cells in mice (17). To explore the possible difference in the functions of $CD11c^{high}$ and $CD11c^{low}$ NK cells, we isolated NK cells from $CD11c^{high}$ or $CD11c^{low}$ group of patients and measured the mRNA levels of representative cytokines IFN-γ and IL-5 as well as corresponding transcription factors T-bet and GATA-3. As shown in Fig. 3, mRNA expression of both IL-5 and GATA-3 was significantly higher in $CD11c^{low}$ MS compared with HS or $CD11c^{high}$ MS, indicating that NK2 bias thought to be characteristic of MS remission is restricted to $CD11c^{low}$ MS. In contrast, there were no differences in mRNA expression of IFN-γ and T-bet among these three groups. Because NK cells from $CD11c^{high}$ patients expressed HLA-DR most brightly, we speculate that NK2 bias associated with $CD11c^{low}$ MS would attenuate when NK cells are further activated or differentiated.

NK cell stimulatory proinflammatory cytokines induce up-regulation of CD11c

We next attempted to explore the mechanism(s) for up-regulation of CD11c on NK cells in $CD11c^{high}$ MS. Because both NK cells and $CD4^+$ T cells overexpressed HLA-DR in $CD11c^{high}$, is it probable that immune signals influencing both innate and acquired immunity are operative. So we hypothesized that cytokine signals that have been implicated in the pathogenesis of MS may play a role. We cultured NK cells from HS in the presence or absence of cytokine(s) for 3 days, and evaluated the CD11c expression (MFI). We focused our attention to IL-12, IL-15, and IL-18, which are known to stimulate NK cells with or without help of other cytokines. Notably, they are reportedly elevated in the serum or blood lymphocytes of MS patients as compared with HS (11–14, 18, 19), and prior studies suggest that they may play an important role in autoimmune diseases (20–24). As shown in Fig. 4, although IL-12 and IL-18 showed only a marginal effect on purified NK cells, IL-15 consistently induced 2- to 3-fold up-regulation of CD11c compared with control culture without addition of cytokines. As IL-12 and IL-18 were reported to synergistically work in various settings (25, 26), we then examined whether combinations of these cytokines may induce CD11c. Combination of IL-15 and IL-12 or of IL-15 and IL-18 did not augment the CD11c expression to the level higher than that could be induced by IL-15 alone. However, the combination of IL-12 and IL-18 did up-regulate CD11c on NK cells, which was comparable to the effect of IL-15 alone (Table I). Additionally, we tested the effects of several cytokines involved in differentiation of DC (TNF-α, GM-CSF, IL-4) (27), or known to up-regulate CD11c in granulocytes (IL-8) as controls (28) in the same assay. These cytokines showed no significant effect (Table I).

$CD11c^{high}$ MS relapsed earlier

Given the significant difference in activation status and cytokine phenotype of NK cells as well as HLA-DR expression by $CD4^+$ T cells, it was particularly interesting to know whether $CD11c^{low}$ and $CD11c^{high}$ MS may follow a different clinical course. A new cohort of

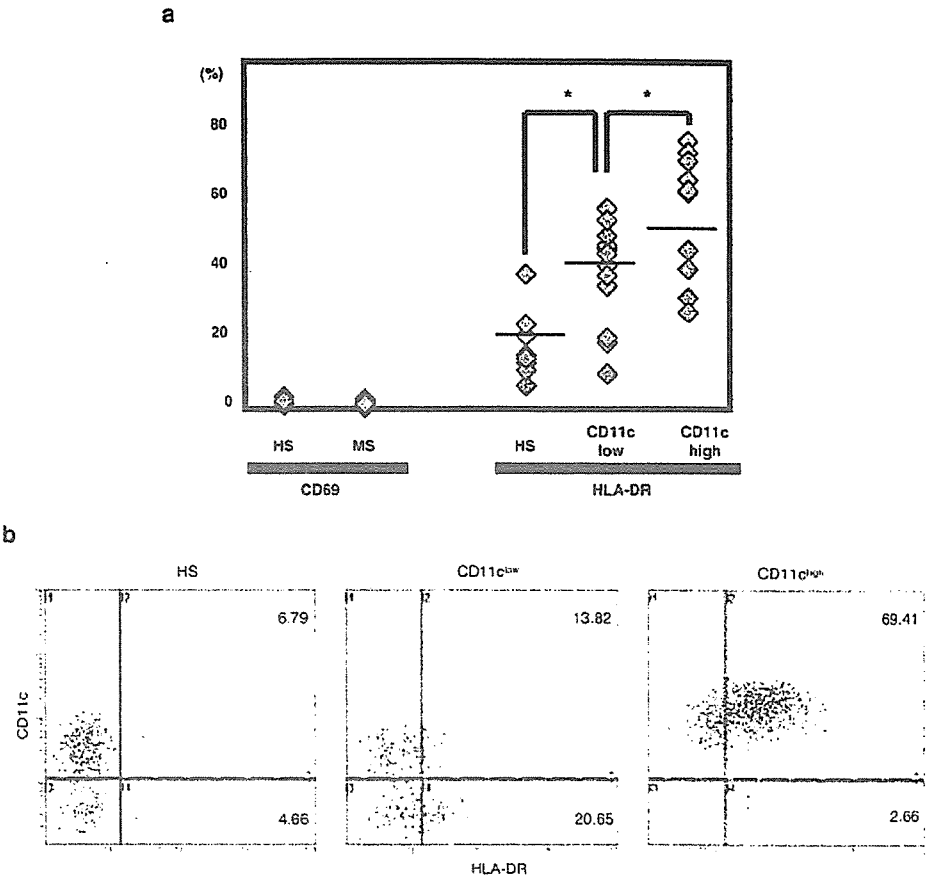

FIGURE 2. Proportions of HLA-DR$^+$ NK cells increase in CD11c^{high} MS. *a*, CD69 and HLA-DR expression on NK cells (CD3$^-$ CD56$^+$ cells). Data are expressed as proportions (percent) of CD69$^+$ cells (7 HS and 16 MS patients in remission) or HLA-DR$^+$ cells (10 HS and 25 MS patients) within whole NK cells. The Student *t* test was used for statistical analysis. Horizontal bars indicate the mean values. *, $p < 0.05$. *b*, Representative expression patterns of HLA-DR vs CD11c on NK cells from a healthy subject (*left*), CD11c^{low} MS (*middle*), and CD11c^{high} MS (*right*).

13 CD11c^{low} and 10 CD11c^{high} MS patients listed in Table II were followed for up to 120 days. In this preliminary exploration, we set the first episode of relapse after blood sampling as an end point. When the neurologist prescribed corticosteroids without knowing any information on the NK cell phenotype, the patient was considered as the dropout at that time point. Remission rate was calculated as Kaplan-Meier survival rate, and statistical difference between CD11c^{low} and CD11c^{high} MS was evaluated with the log-rank test (Fig. 5*a*). At entry, there was no significant difference in the age and disease duration between CD11c^{low} and CD11c^{high} MS (Table II). On analyzing the collected data after completing the study, we found that 8 patients developed a single relapse during the observation period and that the proportion of patients who have had relapse during the follow-up period was greatly higher in CD11c^{high} MS (6 of 10, 60%) than in CD11c^{low} MS (2 of 13, 15.3%). Furthermore, the log-rank test revealed that CD11c^{high} MS relapsed significantly earlier than CD11c^{low} MS ($p = 0.003$), suggesting a possible role of CD11c as a temporal marker for predicting relapse within months after examination. We also explored whether the difference between CD11c^{high} and CD11c^{low} could be influenced by age or sex. When we selected a group of patients younger than 38.5 years old (the mean age of all the patients), a significantly earlier relapse in CD11c^{high} than CD11c^{low} MS was confirmed in this group of patients ($p = 0.0067$, Fig. 5*b*). In the rest of the patients (<38.5 years old), the difference was less clear and not significant ($p = 0.095$). In female patients, CD11c^{high} MS relapsed significantly earlier than CD11c^{low} MS ($p = 0.035$, Fig. 5*c*), whereas this tendency was not statistically significant in male patients ($p = 0.083$). By examining the patients' medical records, we also found that the duration from the last relapse tended to be shorter in CD11c^{high} than CD11c^{low} MS (14.7 ± 12 mo in CD11c^{high} vs 26.7 ± 24.3 mo in CD11c^{low}) and that the mean number of relapses per year was higher in CD11c^{high} MS (0.9 ± 0.6 in CD11c^{high} vs 0.5 ± 0.5 in CD11c^{low}). These are consistent with the postulate that CD11c^{high} MS might be immunologically more active than CD11c^{low} MS (Table II).

Alteration of CD11c expression in the course of MS

We previously described that NK cells may lose NK2 phenotype during relapse (3). It is interesting to know whether the CD11c phenotype also changes in the course of MS. During the follow-up period of 120 days, 8 patients developed a relapse. We were able to take blood samples at relapse before treatment with corticosteroid and then compared the relapse samples with the samples obtained during remission at initiation of the study. As shown in Fig. 6, we saw an obvious tendency that the levels of CD11c expression would decline during relapse ($p < 0.05$). HLA-DR expression on NK cells was also reduced in some patients during relapse, but the difference between remission and relapse samples was not statistically significant.

Expression pattern of CD95 vs CD11c on NK cells in MS

In a previous study, we showed that MS patients could be divided into CD95^{high} and CD95^{low} according to the frequency of CD95$^+$ cells among NK cells (4). Additionally, we examined whether expression of CD11c and CD95 may independently reflect the status of MS. We found no significant correlation between CD95 (%) and CD11c (MFI) on NK cells in MS ($r = 0.29$, $p = 0.16$ with Spearman's correlation coefficient by rank test), indicating that expression of CD95 and CD11c on NK cells may be regulated independently. By setting the upper limits of CD95$^+$ (%) and CD11c MFI as (the average + 2 × SD) of HS (CD95: 44.6%, CD11c: 5.04),

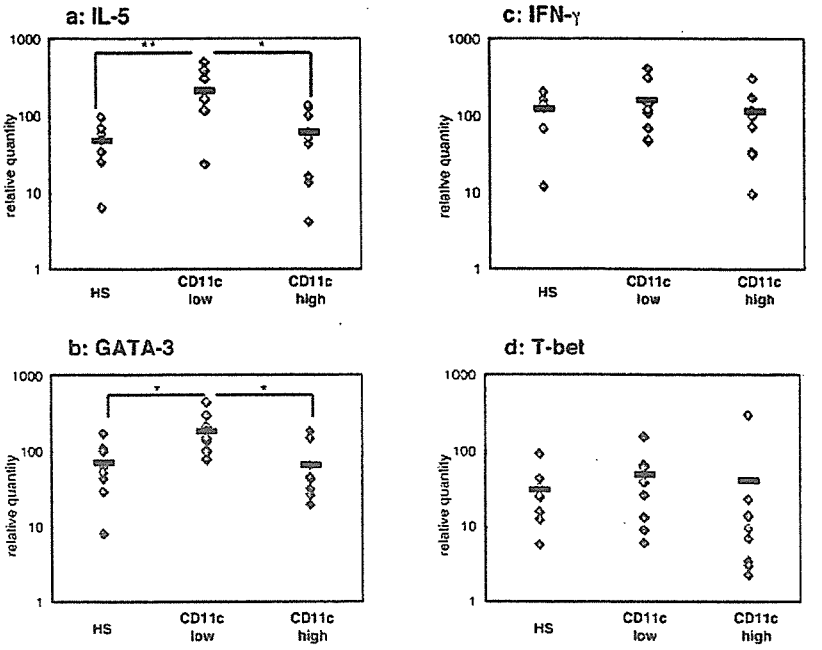

FIGURE 3. IL-5 and GATA-3 mRNA are increased in $CD11c^{low}$ but not in $CD11c^{high}$ MS. Total RNAs were extracted from purified NK cells of HS (n = 8), $CD11c^{low}$ (n = 9), or $CD11c^{high}$ MS (n = 8). mRNA expression of IL-5 (*a*), GATA-3 (*b*), IFN-γ (*c*), and T-bet (*d*) was evaluated by quantitative PCR. The data are normalized to endogenous β-actin expressions in the same samples. ANOVA was used for statistical analysis. Horizontal bars indicate the mean values. *, $p < 0.05$; **, $p < 0.01$.

we then examined whether there is a correlation between CD11c CD95 phenotype and clinical conditions (Fig. 7). Naturally, all the healthy subjects were plotted in the *left lower quadrant* ($CD95^{low}CD11c^{low}$). In contrast, MS patients were plotted in all the four quadrants with differential proportions of patients who have no relapse during 120 days: $CD95^{low}CD11c^{low}$; 3/3 (100%), $CD95^{low}CD11c^{high}$; 1/2 (50%), $CD95^{high}CD11c^{low}$; 8/10 (80%), $CD95^{high}CD11c^{high}$; 2/7 (28.6%). Although the data for $CD95^{low}$ subjects (*lower left* and *lower right*) need to be omitted due to the limited sample size, we found that the difference between $CD95^{high}CD11c^{low}$ and $CD95^{high}CD11c^{high}$ in remission rate was significant with log-rank test (p = 0.028). Provided that $CD95^{high}$ patients possessed an increased frequency of memory autoreactive T cells (4), this result is consistent with the idea that when comparable numbers of autoimmune T cells are present in the peripheral circulation, remission of MS is more stable in patients with $CD11c^{low}$ NK cells.

Discussion

Blood examination of systemic autoimmune diseases such as systemic lupus erythematosus usually exhibits measurable abnormalities such as elevation of autoantibodies, which is useful for evaluating activity of disease. In contrast, patients with MS do not accompany such systemic abnormalities in laboratory tests except

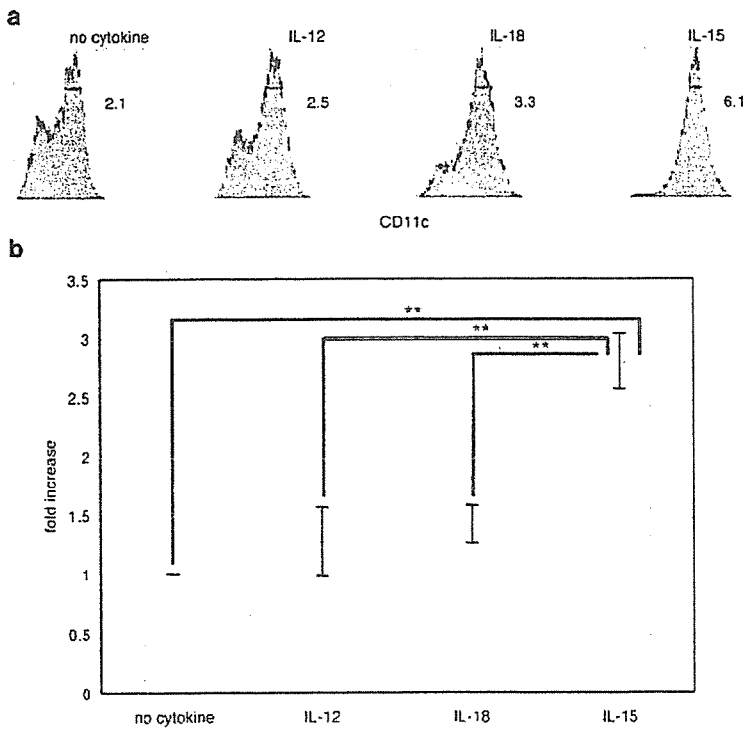

FIGURE 4. CD11c expression on NK cells is upregulated with addition of IL-15. *a*, Purified NK cells were cultured in the absence or presence of IL-12, IL-18, or IL-15. Three days later, the cells were stained with anti-CD11c-PE, -CD3-ECD, and -CD56-PC5 mAb. CD11c expression on NK cells ($CD3^-CD56^+$ cells) is demonstrated as single histogram. Values indicate CD11c MFI of $CD11c^+$ fractions. A representative of three independent experiments is shown. *b*, Data are expressed as mean fold increase of CD11c MFI (the MFI in the presence of cytokine/the MFI in the absence of cytokine) ± SD from three independent experiments. ANOVA was used for statistical analysis. **, $p < 0.01$.

Table I. *Effect of several cytokines on CD11c expression on NK cells*

	No Cytokine	IL-12	IL-18	IL-15	IL-12 + IL-18	IL-4	TNF	GM-CSF	IL-23	IL-8
Expt. 1	1.00[a]	1.19	1.57	**2.90**	ND	ND	ND	ND	ND	ND
Expt. 2	1.00	1.04	1.43	**2.96**	**2.86**	ND	ND	ND	ND	ND
Expt. 3	1.00	1.59	1.25	**2.53**	**3.44**	ND	ND	ND	ND	ND
Expt. 4	1.00	ND	ND	**2.62**	ND	1.19	1.10	0.95	1.14	ND
Expt. 5	1.00	ND	ND	**2.81**	ND	1.24	ND	1.05	1.05	1.00
Mean	1.00	1.27	1.42	**2.77**	**3.15**	1.21	1.10	1.00	1.10	1.00
SD	0.00	0.29	0.16	0.19	0.41	0.03		0.07	0.07	

[a] Purified NK cells were stimulated with cytokines. Data are expressed as fold increase of CD11c MFI (the MFI in the presence of the indicated cytokines/the MFI in the absence of cytokines) in the presence of indicated cytokines. More than a 2-fold increase is highlighted (bold).

in unusual cases. It is currently recognized that autoreactive T cells might be activated and expanded to various degrees in the peripheral blood and peripheral lymphoid organs of MS even during remission (1–4). In fact, our previous work suggests that a higher number of memory autoreactive T cells is linked with unstable disease course (4). If we are able to accurately evaluate the immune status of each patient with a relatively simple test, it should be most helpful in treatment and management of MS. In this line, it is currently of particular importance to identify measurable indicators which would serve as clinically appropriate biomarkers in MS (2).

This study has clarified for the first time to our knowledge that CD11c expression on peripheral NK cells is significantly up-regulated in a major proportion of patients with MS in remission. To obtain insights into the mechanism and the biological meaning of the NK cell expression of CD11c in autoimmune disease MS, we have attempted to clarify the difference between $CD11c^{high}$ and $CD11c^{low}$ patients regarding phenotypes of NK cells, cytokine profile, and temporal clinical activity. We also explored which inflammatory cytokines might induce CD11c on NK cells. According to the NK cell expression of CD11c, we have classified the patients with MS in remission into $CD11c^{high}$ and $CD11c^{low}$. Most notably, NK2 phenotype characterized by predominant IL-5 production was seen in $CD11c^{low}$ patients, but not in $CD11c^{high}$. Consistently, the $CD11c^{high}$ patients were found to be clinically more active than $CD11c^{low}$ as judged by the remission rate during the 120 days after examination. These results indicate that up-regulation of CD11c on NK cells would reflect the temporal disease activity and therefore could be used to identify patients who are likely to exacerbate within months. It has been reported that $CD11c^{+}$ NK cells in mice could serve as APCs (6, 7). However, we could not reveal Ag presenting capacity of human $CD11c^{+}$ NK cells (data not shown).

Regarding the mechanism of CD11c induction on NK cells, we have found that in $CD11c^{high}$ patients, HLA-DR is concomitantly up-regulated with CD11c on NK cells (Fig. 2), which suggests that up-regulation of CD11c may represent an activation-induced change. After exploring the culture condition that may induce CD11c on NK cells, we have found that the addition of IL-15 or combination of IL-12 and IL-18 would increase the expression levels of CD11c on NK cells from healthy individuals. Because increased levels of these proinflammatory cytokines are detected in the blood samples of MS (11–13, 18, 19, 23), it is possible that in

Table II. *Information on the patients whose clinical courses were followed for up to 120 days*

Identification No.	Group	Age (years)	Sex	Disease Period (Years)	Total Number of Relapses	Duration from the Last Relapse (mo)	Mean Numbers of Relapse/Year
1	Low	17	F[a]	9.6	2	24	0.2
2	Low	52	M	12.2	9	3	0.7
3	Low	31	F	6.2	13	7	2.1
4	Low	32	F	3.9	1	34	0.3
5	Low	42	F	2.2	1	8	0.5
6	Low	35	M	20	3	88	0.2
7	Low	37	M	8.5	3	50	0.4
8	Low	35	F	2.4	1	38	0.4
9	Low	26	F	4.8	2	10	0.4
10	Low	26	F	1.5	1	8	0.7
11	Low	41	M	5.5	1	24	0.2
12	Low	64	F	4.5	2	8	0.4
13	Low	42	F	6.3	1	45	0.2
Mean + SD		36.9 + 12.0		6.7 + 5.0	3.1 + 3.7	26.7 + 24.3	0.5 + 0.5
14	High	39	M	4.4	2	22	0.5
15	High	31	F	9.2	11	14	1.2
16	High	46	F	7.4	>20[b]	2	ND
17	High	53	F	2.1	4	5	1.9
18	High	59	F	4.9	2	19	0.4
19	High	27	M	9.3	4	9	0.4
20	High	36	F	2.7	1	19	0.4
21	High	34	F	3.8	2	43	0.5
22	High	60	F	3.4	6	10	1.8
23	High	21	F	1.8	2	4	1.1
		40.6 + 13.4		4.9 + 2.8	3.8 + 3.1	14.7 + 12.0	0.9 + 0.6

[a] F, Female; M, male.
[b] This value is eliminated from calculation of the mean.

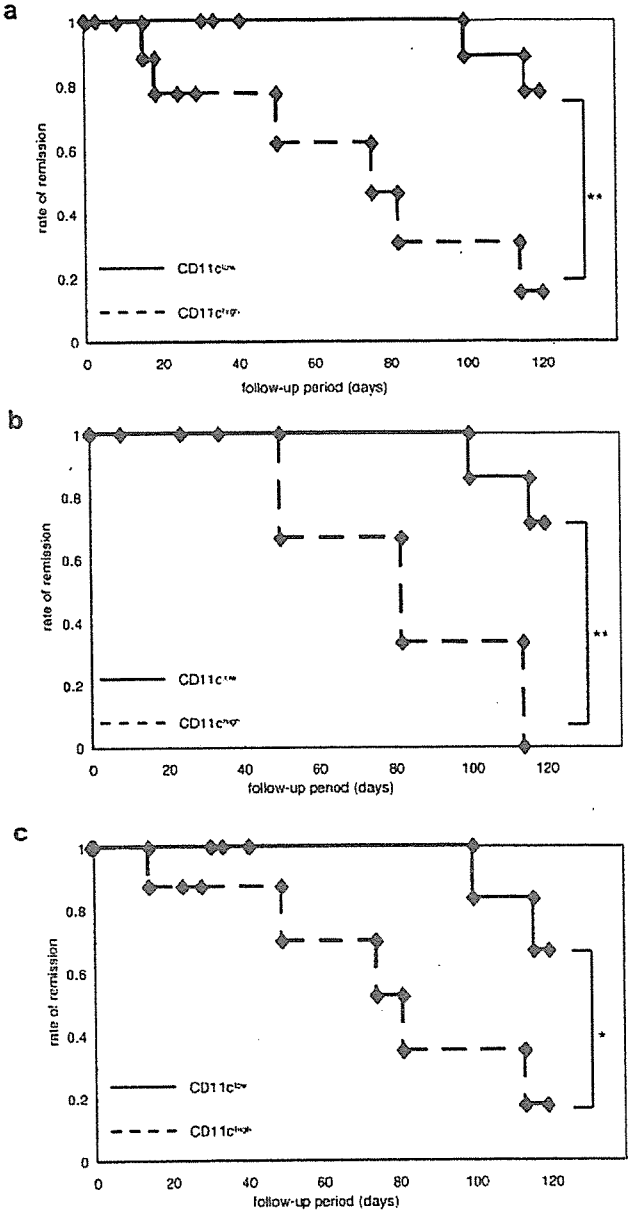

FIGURE 5. Rate of remission is lower in CD11c^{high} MS. The first episode of relapse after blood sampling was set as an end point and clinical course of each patient was followed for up to 120 days. The remission rate was calculated in all (*a*), the younger (*b*), or female (*c*) patients as Kaplan-Meier survival rate, and statistical difference between CD11c^{low} and CD11c^{high} MS was evaluated with log-rank test at day 120. *, $p < 0.05$; **, $p < 0.01$.

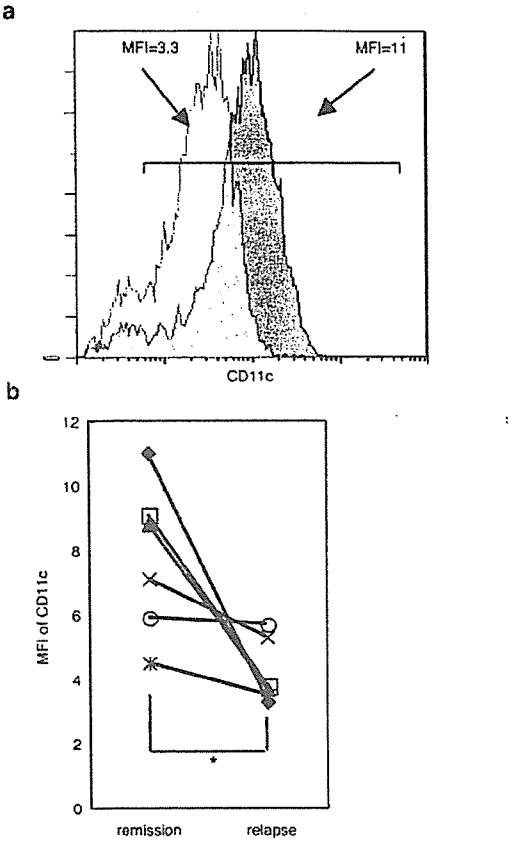

FIGURE 6. Down-regulation of CD11c expression during relapse. *a*, Representative CD11c histograms from the same patient in remission (closed) and relapse (open). Values indicate CD11c MFI of CD11c$^+$ fractions. *b*, Comparison of NK cells from remission and relapse from the same patients ($n = 6$). The data obtained from the same patients are connected with lines. Wilcoxon signed-ranks test was used for statistical analysis. *, $p < 0.05$.

vitro CD11c induction on NK cells may recapitulate the phenotypic alteration of NK cells in CD11c^{high} patients. Interestingly, IL-18 is not only a cytokine able to facilitate IFN-γ production by NK cells in cooperation with IL-12 (25, 26) but is crucial in inducing pathogenic autoimmune responses (21). Furthermore, autoimmune encephalitogenic T cells can induce more serious disease upon adoptive transfer when they are preactivated in the presence of IL-12 and IL-18 (20). Taken together, these results allow us to speculate that the proinflammatory cytokines may be involved in the up-regulation of CD11c on NK cells. Although the relationship between serum cytokine concentration and levels of CD11c expression on NK cells should be estimated in future studies, a previous work (11, 29, 30) showing that a probable link between IL-15 and temporal disease activity, indicates that NK cell expression of CD11c is likely to correlate with the levels of cytokines.

In the Th cell differentiation, specific transcription factors have been identified that play a crucial role in inducing Th1 or Th2 cells. Namely, Th1 differentiation characterized by IFN-γ induction requires a transcription factor T-bet, whereas GATA-3 and c-*maf* act to promote Th2 cytokine production (31–33). Human NK cells cultured in the presence of IL-12 or IL-4 differentiate into NK1 or NK2 populations, reminiscent of Th1 and Th2 cells (5). Whereas NK1 cells produce IL-10 and IFN-γ, NK2 cells would serve as immune regulators by producing IL-5 and IL-13. Notably, up-regulation of GATA-3 has been reported in mouse NK2 cells (17), raising a possibility that Th cells and NK cells might share the same transcription factor for inducing the key cytokine. We have previously reported that IL-5 expression is one of the characteristics of NK cells in the remission state of MS (3). However, it was not excluded that overexpression of IL-5 could be restricted to a proportion of the patients. Here, we have addressed whether NK cells from CD11c^{high} and CD11c^{low} may differ with regard to expression levels of IFN-γ and IL-5 and of their transcription factors T-bet and GATA-3. By measuring the mRNAs, we found that expression levels of IL-5 and GATA-3 are elevated in CD11c^{low} MS but not in CD11c^{high} (Fig. 3). Furthermore, we showed that

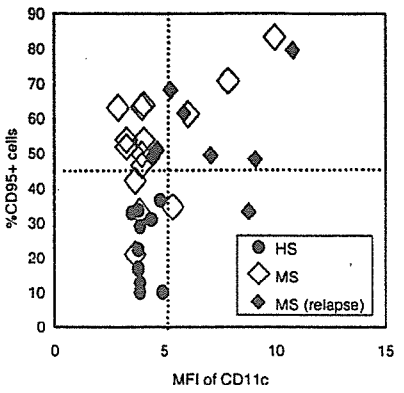

FIGURE 7. Expression pattern of CD95 vs CD11c on NK cells from MS. PBMC from MS or HS were stained with CD95-FITC, CD11c-PE, CD3-ECD, and CD56-PC5. After determining the proportion of $CD95^+$ cells among NK cells and CD11c expression (MFI) of CD11c, we plotted each patient according to the obtained values. Dotted lines represent the upper limits of $CD95^+$ cell (percent) and CD11c MFI for HS as (the average + two times SD) of HS. ●, HS; ◇, MS; ◆, MS patients who relapsed during the 120 days follow-up period.

neither IFN-γ nor T-bet was increased in $CD11c^{high}$ MS. This suggests that NK cells from $CD11c^{low}$ are NK2-biased but those from $CD11c^{high}$ are not, although MS in remission as a whole is NK2-biased as compared with control subjects. More recently, we have observed that stimulation with IL-15 or IL-12 plus IL-18 would decrease IL-5 and GATA-3 mRNA in purified NK cells with reciprocal up-regulation of CD11c (data not shown). This further supports a model that proinflammatory cytokines may play a crucial role in the absence of NK2 bias in $CD11c^{high}$ MS.

To clarify the clinical differences between $CD11c^{high}$ and $CD11c^{low}$, we followed up the clinical course of the patients after blood sampling. Although there was no significant difference in clinical parameters at examination of NK cells, we have found that $CD11c^{high}$ MS showed a significantly earlier relapse than $CD11c^{low}$ MS. This is consistent with our assumption that the absence of NK2 bias in $CD11c^{high}$ MS should imply that regulatory NK cell functions are defective in this group of patients. When we reanalyzed the data regarding various clinical parameters, we found that an earlier relapse in $CD11c^{high}$ than $CD11c^{low}$ MS is more remarkable in the younger group (<38.5 years old) or in female patients. Furthermore, the duration from the last relapse tended to be shorter and the mean number of relapses per year higher in $CD11c^{high}$ MS, supporting that $CD11c^{high}$ MS is more active than $CD11c^{low}$ MS.

When we analyzed expression of CD95 and CD11c on NK cells simultaneously, we found that MS patients in remission could be divided into four subgroups (Fig. 7). When we compared clinical course after examination of NK cell phenotypes, we found that $CD95^{high}CD11c^{high}$ MS relapsed significantly earlier than $CD95^{high}CD11c^{low}$ MS ($p = 0.028$ with log-rank test). This result indicates that $CD95^{high}CD11c^{high}$ MS may be most unstable subgroup of MS, among the patients whose clinical state could be judged as being in clinical remission.

In this study, we have demonstrated that MS patients differentially express CD11c on peripheral blood NK cells and a higher expression of CD11c on NK cells may reflect the temporal disease activity as well as functional alteration of regulatory NK cells. Our results have a clinical implication because of a lack of appropriate biomarker to monitor the immunological status in MS at present. To verify the reliability of this marker, longitudinal examination of CD11c expression on NK cells in the same patients should be performed in the future study.

Disclosures

The authors have no financial conflict of interest.

References

1. Sospedra, M., and R. Martin. 2005. Immunology of multiple sclerosis. *Annu. Rev. Immunol.* 23: 683–747.
2. Bielekova, B., and R. Martin. 2004. Development of biomarkers in multiple sclerosis. *Brain* 127: 1463–1478.
3. Takahashi, K., S. Miyake, T. Kondo, K. Terao, M. Hatakenaka, S. Hashimoto, and T. Yamamura. 2001. Natural killer type 2 bias in remission of multiple sclerosis. *J. Clin. Invest.* 107: R23–R29.
4. Takahashi, K., T. Aranami, M. Endoh, S. Miyake, and T. Yamamura. 2004. The regulatory role of natural killer cells in multiple sclerosis. *Brain* 127: 1917–1927.
5. Perini, D., S. Robertson, G. Gri, L. Showe, M. Aste-Amezaga, and G. Trinchieri. 1998. Differentiation of human NK cells into NK1 and NK2 subsets. *J. Immunol.* 161: 5821–5824.
6. Homann, D., A. Jahreis, T. Wolfe, A. Hughes, B. Coon, M. J. van Stipdonk, K. R. Prilliman, S. P. Schoenberger, and M. G. von Herrath. 2002. CD40L blockade prevents autoimmune diabetes by induction of bitypic NK/DC regulatory cells. *Immunity* 16: 403–415.
7. Pillarisetty, V. G., S. C. Katz, J. I. Bleier, A. B. Shah, and R. P. Dematteo. 2005. Natural killer dendritic cells have both antigen presenting and lytic function and in response to CpG produce IFN-γ via autocrine IL-12. *J. Immunol.* 174: 2612–2618.
8. Bilsland, C. A., M. S. Diamond, and T. A. Springer. 1994. The leukocyte integrin p150,95 (CD11c/CD18) as a receptor for iC3b: activation by a heterologous β subunit and localization of a ligand recognition site to the I domain. *J. Immunol.* 152: 4582–4589.
9. Stacker, S. A., and T. A. Springer. 1991. Leukocyte integrin P150,95 (CD11c/CD18) functions as an adhesion molecule binding to a counter-receptor on stimulated endothelium. *J. Immunol.* 146: 648–655.
10. Morelli, A. E., A. T. Larregina, W. J. Shufesky, A. F. Zahorchak, A. J. Logar, G. D. Papworth, Z. Wang, S. C. Watkins, L. D. Falo, Jr., and A. W. Thomson. 2003. Internalization of circulating apoptotic cells by splenic marginal zone dendritic cells: dependence on complement receptors and effect on cytokine production. *Blood* 101: 611–620.
11. Blanco-Jerez, C., J. F. Plaza, J. Masjuan, L. M. Orensanz, and J. C. Alvarez-Cermeno. 2002. Increased levels of IL-15 mRNA in relapsing-remitting multiple sclerosis attacks. *J. Neuroimmunol.* 128: 90–94.
12. Huang, W. X., P. Huang, and J. Hillert. 2004. Increased expression of caspase-1 and interleukin-18 in peripheral blood mononuclear cells in patients with multiple sclerosis. *Mult. Scler.* 10: 482–487.
13. Balashov, K. E., D. R. Smith, S. J. Khoury, D. A. Hafler, and H. L. Weiner. 1997. Increased interleukin 12 production in progressive multiple sclerosis: induction by activated $CD4^+$ T cells via CD40 ligand. *Proc. Natl. Acad. Sci. USA* 94: 599–603.
14. Karni, A., D. N. Koldzic, P. Bharanidharan, S. J. Khoury, and H. L. Weiner. 2002. IL-18 is linked to raised IFN-γ in multiple sclerosis and is induced by activated $CD4^+$ T cells via CD40-CD40 ligand interactions. *J. Neuroimmunol.* 125: 134–140.
15. McDonald, W. I., A. Compston, G. Edan, D. Goodkin, H. P. Hartung, F. D. Lublin, H. F. McFarland, D. W. Paty, C. H. Polman, S. C. Reingold, et al. 2001. Recommended diagnostic criteria for multiple sclerosis: guidelines from the International Panel on the diagnosis of multiple sclerosis. *Ann. Neurol.* 50: 121–127.
16. Lima, M., J. Almeida, M. dos Anjos Teixeira, M. L. Queiros, B. Justica, and A. Orfao. 2002. The "ex vivo" patterns of CD2/CD7, CD57/CD11c, CD38/CD11b, CD45RA/CD45RO, and CD11a/HLA-DR expression identify acute/early and chronic/late NK-cell activation states. *Blood Cells Mol. Dis.* 28: 181–190.
17. Katsumoto, T., M. Kimura, M. Yamashita, H. Hosokawa, K. Hashimoto, A. Hasegawa, M. Omori, T. Miyamoto, M. Taniguchi, and T. Nakayama. 2004. STAT6-dependent differentiation and production of IL-5 and IL-13 in murine NK2 cells. *J. Immunol.* 173: 4967–4975.
18. Nicoletti, F., R. Di Marco, K. Mangano, F. Patti, E. Reggio, A. Nicoletti, K. Bendtzen, and A. Reggio. 2001. Increased serum levels of interleukin-18 in patients with multiple sclerosis. *Neurology* 57: 342–344.
19. Fassbender, K., A. Ragoschke, S. Rossol, A. Schwartz, O. Mielke, A. Paulig, and M. Hennerici. 1998. Increased release of interleukin-12p40 in MS: association with intracerebral inflammation. *Neurology* 51: 753–758.
20. Ito, A., A. Matejuk, C. Hopke, H. Drought, J. Dwyer, A. Zamora, S. Subramanian, A. A. Vandenbark, and H. Offner. 2003. Transfer of severe experimental autoimmune encephalomyelitis by IL-12- and IL-18-potentiated T cells is estrogen sensitive. *J. Immunol.* 170: 4802–4809.
21. Shi, F. D., K. Takeda, S. Akira, N. Sarvetnick, and H. G. Ljunggren. 2000. IL-18 directs autoreactive T cells and promotes autodestruction in the central nervous system via induction of IFN-γ by NK cells. *J. Immunol.* 165: 3099–3104.
22. Takeda, K., H. Tsutsui, T. Yoshimoto, O. Adachi, N. Yoshida, T. Kishimoto, H. Okamura, K. Nakanishi, and S. Akira. 1998. Defective NK cell activity and Th1 response in IL-18-deficient mice. *Immunity* 8: 383–390.

23. Makhlouf, K., H. L. Weiner, and S. J. Khoury. 2001. Increased percentage of IL-12$^+$ monocytes in the blood correlates with the presence of active MRI lesions in MS. *J. Neuroimmunol.* 119: 145–149.
24. Waldmann, T. A. 2004. Targeting the interleukin-15/interleukin-15 receptor system in inflammatory autoimmune diseases. *Arthritis Res. Ther.* 6: 174–177.
25. Fehniger, T. A., M. H. Shah, M. J. Turner, J. B. VanDeusen, S. P. Whitman, M. A. Cooper, K. Suzuki, M. Wechser, F. Goodsaid, and M. A. Caligiuri. 1999. Differential cytokine and chemokine gene expression by human NK cells following activation with IL-18 or IL-15 in combination with IL-12: implications for the innate immune response. *J. Immunol.* 162: 4511–4520.
26. Okamura, H., S. Kashiwamura, H. Tsutsui, T. Yoshimoto, and K. Nakanishi. 1998. Regulation of interferon-γ production by IL-12 and IL-18. *Curr. Opin. Immunol.* 10: 259–264.
27. Young, J. W., P. Szaboles, and M. A. Moore. 1995. Identification of dendritic cell colony-forming units among normal human CD34$^+$ bone marrow progenitors that are expanded by c-*kit*-ligand and yield pure dendritic cell colonies in the presence of granulocyte/macrophage colony-stimulating factor and tumor necrosis factor α. *J. Exp. Med.* 182: 1111–1119.
28. Detmers, P. A., S. K. Lo, E. Olsen-Egbert, A. Walz, M. Baggiolini, and Z. A. Cohn. 1990. Neutrophil-activating protein 1/interleukin 8 stimulates the binding activity of the leukocyte adhesion receptor CD11b/CD18 on human neutrophils. *J. Exp. Med.* 171: 1155–1162.
29. Kivisakk, P., D. Matusevicius, B. He, M. Soderstrom, S. Fredrikson, and H. Link. 1998. IL-15 mRNA expression is up-regulated in blood and cerebrospinal fluid mononuclear cells in multiple sclerosis (MS). *Clin. Exp. Immunol.* 111: 193–197.
30. Pashenkov, M., M. Mustafa, P. Kivisakk, and H. Link. 1999. Levels of interleukin-15-expressing blood mononuclear cells are elevated in multiple sclerosis. *Scand. J. Immunol.* 50: 302–308.
31. Szabo, S. J., S. T. Kim, G. L. Costa, X. Zhang, C. G. Fathman, and L. H. Glimcher. 2000. A novel transcription factor, T-bet, directs Th1 lineage commitment. *Cell.* 100: 655–669.
32. Szabo, S. J., B. M. Sullivan, C. Stemmann, A. R. Satoskar, B. P. Sleckman, and L. H. Glimcher. 2002. Distinct effects of T-bet in TH1 lineage commitment and IFN-γ production in CD4 and CD8 T cells. *Science* 295: 338–342.
33. Zheng, W., and R. A. Flavell. 1997. The transcription factor GATA-3 is necessary and sufficient for Th2 cytokine gene expression in CD4 T cells. *Cell* 89: 587–596.

Available online at www.sciencedirect.com
SCIENCE DIRECT
ELSEVIER
European Journal of Medicinal Chemistry 41 (2006) 569–576
EUROPEAN JOURNAL OF MEDICINAL CHEMISTRY
http://france.elsevier.com/direct/ejmech

Original article

Induction of promotive rather than suppressive immune responses from a novel NKT cell repertoire Vα19 NKT cell with α-mannosyl ceramide analogues consisting of the immunosuppressant ISP-I as the sphingosine unit

Michio Shimamura [a,*], Naoki Okamoto [a], Yi-Ying Huang [a], Jouji Yasuoka [b], Kenji Morita [b], Akira Nishiyama [b], Yuusuke Amano [b], Tadashi Mishina [b]

[a] *Developmental Immunology Unit, Mitsubishi Kagaku Institute of Life Sciences, 11 Minamiooya, Machida, Tokyo 194-8511, Japan*
[b] *Pharmaceuticals Research Division, Mitsubishi Pharma Corporation 1000, Kamoshida-cho, Aoba-Ku, Yokohama 227-0033, Japan*

Received in revised form 10 November 2005; accepted 29 November 2005
Available online 20 March 2006

Abstract

A 2-substituted 2-aminopropane-1,3-diol or 2-aminoethanol is the minimum structure required for the immunosuppressive activity of ISP-I, an antibiotic isolated from the culture broth of *Isaria sinclairil*. A series of α-mannosyl ceramide (α-ManCer) analogues was derived from 2-substituted 2-aminopropane-1,3-diols or 2-aminoethanols in place of sphingosine. The newly synthesized glycosides were evaluated for their effects on immune responses. In contrast to the immunosuppressive activity of the precursors, the α-ManCer analogues induced immunopromotive responses from invariant Vα19-Jα26 transgenic mouse lymphocytes more effectively than the original α-ManCer. Collectively, it is strongly suggested that the 2-substituted 2-aminopropane-1,3-diols and 2-aminoethanols mimic sphingosine in the α-ManCer analogues so that they potentially acquire specific antigenicity toward Vα19 NKT cell, a novel NKT cell subset.

Keywords: NKT cell; immunomodulation; glycosphingolipid

1. Introduction

Natural killer T (NKT) cells are defined as lymphocytes bearing both the common NK marker NKR-P1 and T cell receptors (TCRs) [1,2]. They are characterized by the expression of invariant TCR α chains such as mouse Vα14-Jα18 and human Vα24-JαQ α chains. Recently, we demonstrated the presence of a novel NKT cell repertoire (designated the Vα19 NKT cell) in mice [3]. This repertoire characteristically expressed the Vα19-Jα26 (AV19-AJ33) invariant TCR α chain that was previously found in mammalian peripheral blood [4]. Vα19 NKT cells along with the well characterized invariant Vα14-Jα18 TCR α^+ NKT (Vα14 NKT) cells [5,6] produce large amounts of both Th1- and Th2-promoting immunoregulatory cytokines, upon stimulation of the invariant TCR, and are considered to participate in the regulation of the immune system in mammalians [7,8] (M. Shimamura et al. "Invariant TCR-directed development of Vα19 NKT cell promptly producing immunoregulatory cytokines in response to TCR engagement with glycolipid antigens", manuscript to be submitted.) Therefore, the identification of specific antigens for Vα19 NKT cells is required to develop new therapies for various disorders. We have recently found that α-mannosyl ceramide (α-ManCer) in the context of one of the non-classical MHC class I molecules MR1 [9] specifically stimulates Vα19 NKT cells [8].

Previously, we found immunosuppressive activity by ISP-I [10,11], a product of *Isaria sincliairii* (ATCC 24400) which was later shown to be identical to antifungal and antibiotic

Abbreviations: α-ManCer, α-mannosyl ceramide; MNC, mononuclear cell; Vα19, NKT cell; invariant Vα19-Jα26 TCR α^+, NK1.1$^+$ T cell; Vα14, NKT cell; invariant Vα14-Jα18 TCR α^+, NK1.1$^+$ T cell.

* Corresponding author. Tel.: +81 42 724 6348; fax: +81 42 724 6342.
E-mail address: michio@libra.ls.m-kagaku.co.jp (M. Shimamura).

0223-5234/$ - see front matter © 2006 Elsevier SAS. All rights reserved.
doi:10.1016/j.ejmech.2005.11.013

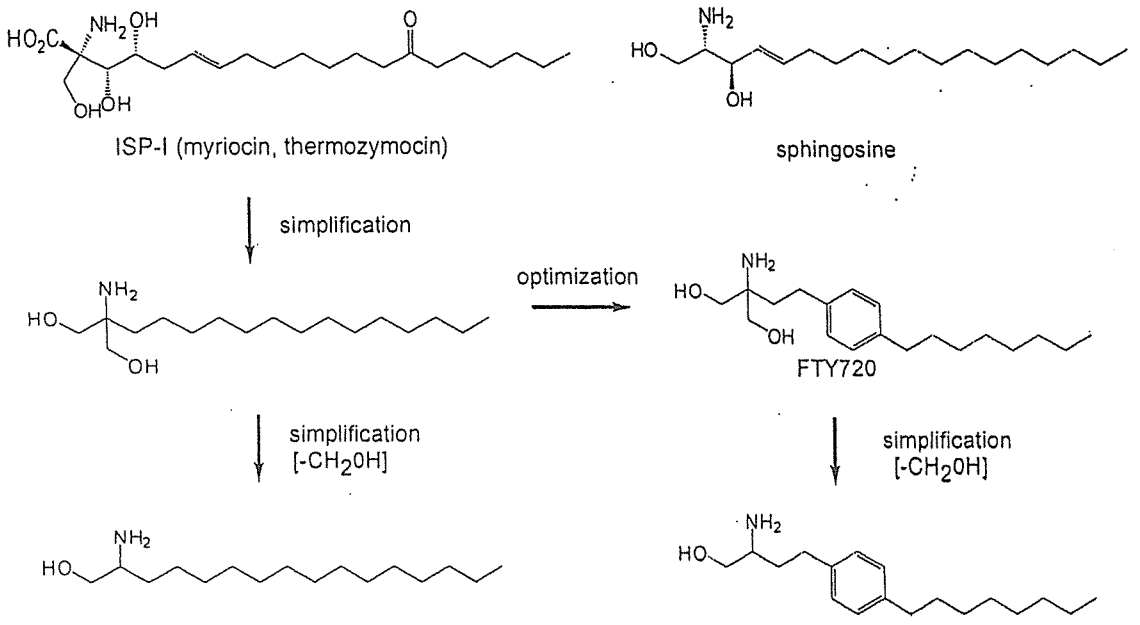

Fig. 1. Immunosuppressive ISP-I and its derivatives compared with sphingosine. ISP-I derivatives simplified and optimized in termed of the immunosuppressive activity were used for the synthesis of α-ManCer analogues.

myriocin [12] or thermzymocidin [13] (Fig. 1). A comprehensive study of the structure-activity relationship of chemically modified derivatives of ISP-I revealed that the 2-amino-1,3-propane diol, especially the 2-aminoethanol moiety, is the structure of ISP-I required for the immunosuppressive activity [10,11]. Furthermore, modification of the hydrophobic portion indicated that the 2-substituted 2-aminoethanol with a 4-octylphenyl group (FTY720) optimized the immunosuppressive potential [10,11] (Fig. 1). Loss of chirality in these compounds facilitated the synthesis. In addition, the derivatives were less cytotoxic than the original ISP-I. As suggested by the structural homology between FTY720 and sphingosine, recent studies have demonstrated that this drug targets sphingosine-1-phosphate receptors and acts as an agonist [14,15].

In the current study, we focused on a series of α-ManCer derivatives in which the sphingosine moiety was replaced with FTY720 and related aminoalcohols (Fig. 1). We found that the modified α-ManCer induced promotive rather than suppressive immune responses from Vα19 NKT cells.

2. Results and discussion

2.1. Synthesis of α-glycosyl ceramide derivatives

It has been found that the immunosuppressive activity of ISP-I involves the moiety of 2-amino-1,3-propanediol, especially 2-aminoethanol [10,11]. The 2-substituted derivatives depicted in Fig. 1 were used as precursors in place of sphingosine, and a series of α-glycosyl ceramide analogues were synthesized.

2-Substituted 2-aminoalcohols (**1**) were *N*-acylated with an appropriate length of acylchrolide and the resultant amides (**2**) were used as glycosylation acceptors (Scheme 1A). Similarly, glycosylation acceptors were synthesized from 2-substituted 2-amino-1,3-propanediols (**3**) (Scheme 2). One of the two hydroxymethyl groups of **3** was protected with triethyl orthoacetate to afford **4** at first. The remaining hydroxymethyl group of **4** was benzylated (**5**). Then, the oxazoline ring of **5** protecting both hydroxymethyl and amino groups was removed (**6**). The amino group was finally *N*-acylated to give **7a–d**. The resultant *O*-benzylated amides were useful as glycosylation acceptors because the benzyl group was stable during the following glycosylation reaction and was easily separable by hydrogenation afterwards simultaneously with the other benzyl groups protecting the sugar hydroxyl groups. **7a–d** were optically inactive, thus indicating that they are an equivalent mixture in terms of the chirality at the C2 of the sphingosine analogue.

The amides **2** and **7** were next glycosylated with **8** to afford glycosides (**9**) (Scheme 3). The α-anomers were predominantly obtained when 1-fluoro 2,3,4,6-benzyl galactose was used as a glycosilation donor [16]. The α-anomers were similarly the main products when 1-*O*-acetyl 2,3,4,6-benzyl mannose was the glycosylation donor, because the β-glycosylation was hampered by the steric hindrance with the 2-axial *O*-benzyl group during the transition state of the glycosylation reaction. The predominantly formed α anomers were successfully separated from the β anomers by silica gel column chromatography at this stage. Finally, the benzyl protection groups were removed from **9** by reduction and the products (**10**) were obtained.

2.2. Immunological activity of α-glycosyl ceramide analogues

To examine whether α-glycosyl ceramide analogues derived from the immunosuppressants were immunopromotive

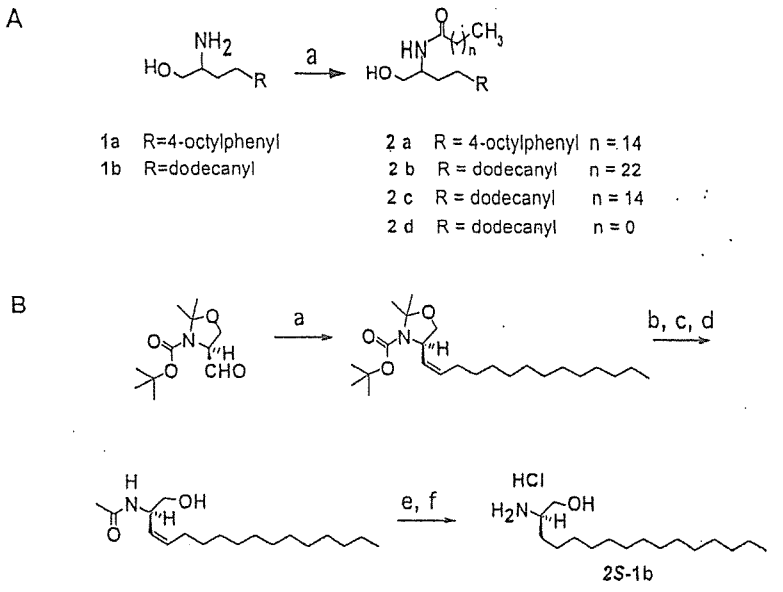

Scheme 1. (A). *N*-Acylation of 2-aminoethanol derivatives used as glycosylation acceptors. (a): Reagents and conditions, Cl C=O–$(CH_2)_n$ CH_3, TMSCl, pyridine. Yield: 2a, 46%; 2b, 25%; 2c, 50%; 2d, 41%. (B). Preparation of the diastereomers of 2-aminohexadecanol. A synthetic pathway of *2S*-1b is shown here. 2R-1b was similarly prepared from the corresponding diastereomer of Garner's aldehyde. (a): $[Ph_3P(CH_2)_{12}CH_3]Br$/n-BuLi/THF. (b): TFA. (c): Ac_2O/pyridine. (d): 2M HCl/THF. (e): H_2, 10% Pd-C/EtOH. (f): Conc.HCl/EtOH.

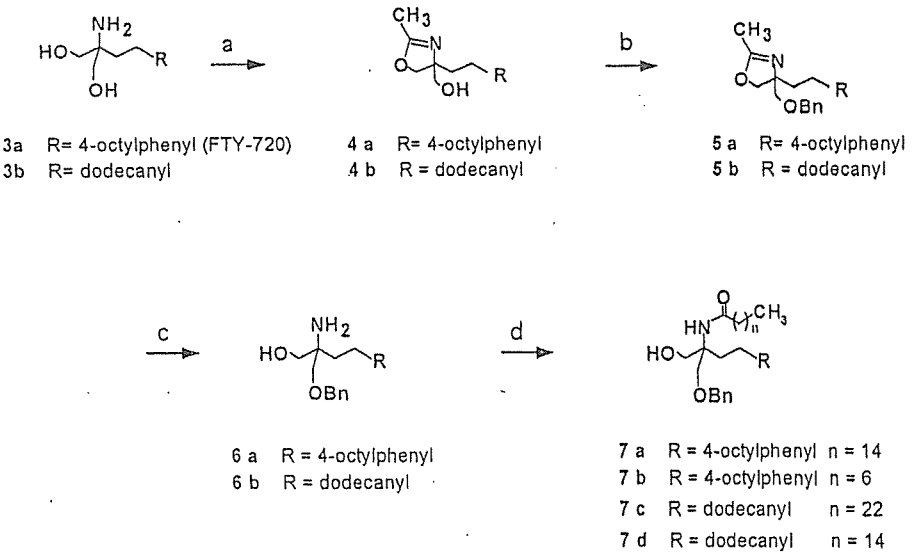

Scheme 2. Synthesis of *N*-acyl 2-amino-1,3-propanediol derivatives used as glycosylation acceptors.
(a): $CH_3C(OEt)_3$, *i*PrN$(Et)_2$, Yield: 81 ~ 87 %, (b): BnBr, NaH, THF, Yield: 41 ~ 49%. (c): Conc. HCl. Yield: 88 ~ 97%. (d): (1) TMS (trimethylsilyl)Cl, pyridine, (2) ClC=O–$(CH_2)_n CH_3$, Yield: 75 ~ 85%.

or suppressive, a series of α-glycosides (Scheme 3) was tested for the effects on mouse lymphocytes. Liver mononuclear cells (MNCs) were prepared from C57BL/6 mice and Vα19-Jα26 invariant TCR α transgenic (Tg) mice [7,8] (with the TCR $\alpha^{-/-}$ background). The C57BL/6 MNCs included 30% invariant Vα14-Jα18 TCR α^+ NKT (Vα14 NKT) cells [17], whereas the Vα19 Tg^+ MNCs included 30% Vα19 NKT cells as the sole NKT cell population [7,8]. These cells were cultured as responders in the presence of the glycolipids. Immune responses were assessed by measurement of cell proliferation and IL-2 secretion in the culture supernatants (Fig. 2). α-ManCer derivatives more or less enhanced proliferation of Vα19 Tg^+ cells and the production of IL-2 irrespective of the modification in the sphingosine portion. *In addition, the derivatives induced activation of spleen cells of the Vα19 Tg+ mice previously primed with them. The spleen cells transferred to culture spontaneously secreted IL-2* (Fig. 3) *and other cytokines (data not shown). These findings strongly suggest that the α-ManCer analogues consisting of the immunosuppressive structural unit as well as intact α-ManCer are immunopromo-*

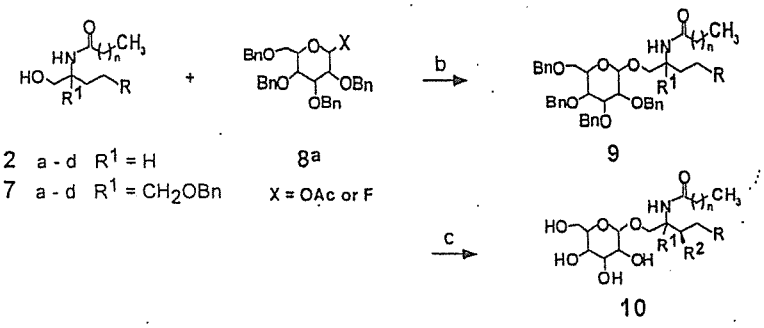

9, 10

	R	R^1	R^2	n	Hexose	Abbreviation
a	4-octylphenyl	H	H	14	α-Man	Man4PhC16
b	dodecanyl	H	H	22	α-Gal	GalC24
c	dodecanyl	H	H	14	α-Man	ManC16
d	dodecanyl	H	H	0	α-Gal	GalC2
e	4-octylphenyl	CH_2OH	H	14	α-Man	Man2HM4PhC16
f	4-octylphenyl	CH_2OH	H	14	α-Gal	Gal2HM4PhC16
g	4-octylphenyl	CH_2OH	H	6	α-Gal	Gal2HM4PhC8
h	dodecanyl	CH_2OH	H	22	α-Man	Man2HMC24
i	dodecanyl	CH_2OH	H	14	α-Man	Man2HMC16
	dodecanyl	H	OH	14	α-Man	Man3OHC16 [d]

Scheme 3. Synthesis of α-glycosyl ceramide derivatives.
(a): 1-*O*-acetyl-2,3,4,6-tetrabenzyl-D-mannose or 1-fluoro-2,3,4,6-tetrabenzyl-D-galactose. (b): BF_3-Et_2O, CH_2Cl_2, for 1-*O*-acetate, $SnCl_2$, $AgClO_4$-H_2O, molecular sieve 4A, Et_2O for 1-fluoride. Yield: 9a, 54%; 9b, 14%; 9c, 66%; 9d, 55%; 9e, 37%; 9f, 74%; 9g, 37%; 9h, 18%; 9i 25%. *The yields of the β-anomers were less than 10%.* (c): H_2, 20%, $Pd(OH)_2$-C, EtOH. Yield: 10a, 33%; 10b, 33%; 10c, 35%; 10d, 39%; 10e, 16%; 10f, 76%; 10g, 53%; 10h, 68%; 10i 81%. (d): Man3OHC16 was synthesized as described previously [8].

tive to Vα19 NKT cells [8]. Above all, Man4PhC16 (**10a**) stimulated Vα19 Tg^+ cells rather intensively compared with ManC16 (**10c**) or the intact α-ManCer (Man3OHC16) in the same concentration (only Man3OHC16 keeps chirality at the C2 of the sphingosine). Vα19 NKT cells recognize the mannosyl residue of α-ManCer when it is presented by the antigen-presenting molecule MRI, one of the non-polymorphic MHC class I-like molecules [8]. Thus, it is suggested that the introduction of a phenyl group in the sphingosine portion in **10a** improved the recognition of the α-mannosyl residue by the invariant Vα19 TCR, presumably arising from the augmented interaction between the modified portion of the sphingosine and the MRI antigen-presenting groove.

As found in α-ManCer [8], α-ManCer analogues had less of an effect on C57BL/6 cells than Vα19 Tg^+ cells. Combined with the finding that NK1.1$^+$ Vα19 Tg^+ cells but not NK1.1$^-$ Vα19 Tg^+ cells were responsive to the glycolipid antigens (Shimamura et al., manuscript to be submitted), it is suggested that the specific recognition of α-ManCer analogues is carried out by Vα19 NKT cells.

α-ManCer analogues synthesized here are an equivalent mixture of diastereomers in terms of the chirality at C2 of modified sphingosine as described above. To determine which form of the diastereomer is immunopromotive to Vα19 NKT cells, both *S* and *R* forms of ManC16 (**10c**) were synthesized by the same method from optically active **1b** (Scheme 1B) and assessed the activity. *2R-10c induced* 1.6 ± 0.3 *fold-increase of cell proliferation of Vα19Tg TCRα$^{-/-}$ liver lymphocytes, whereas 2S-10c caused* 1.1 ± 0.2 *fold-increase. Thus, the 2R-form diastereomer of α-ManCer analogues corresponding to the configuration of naturally occurring sphingosine are likely to primarily responsible for the immunopromotive activity.*

GalC24 (**10b**) was immunopromotive toward C57BL/6 cells. However, this glycolipid was less effective than KRN7000 (α-GalCer consisting of sphingosine-3,4-diol) [18], data not shown). In addition, Gal2HMPhC18 (**10f**) had no significant effect on C57BL/6 cells. These findings indicate a stringent structural restriction in the sphingosine portion of α-GalCer. *Presumably, KRN7000 is properly presented by CDld, so that α-GalCer is recognized as an effective antigen by invariant Vα14-Jα18 TCR$^+$ NKT cells* [18]. α-GalCer analogues with a short *N*-acyl chain (GalC2 (**10d**) and Gal2HM4PhC8 (**10g**)) suppressed the immune responses of both C57BL/6 and Vα19 Tg^+ lymphocytes, suggesting that two suitably long hydrocarbon chains are necessary for antigenic glycosyl ceramides to properly fit to the groove of CDld [19,20] or MRI.

3. Conclusion

Modified α-ManCers consisting of an immunosuppressive sphingosine analogue were promotive rather than suppressive of the immune responses by Vα19 NKT cell. Some of them were more immunopromotive than the original α-ManCer. This suggests that the structural modification in the sphingosine moiety in α-ManCer improves the space location of the α-mannosyl residue to be recognized by the invariant Vα19 TCR. More functional glycolipids should be obtained on the

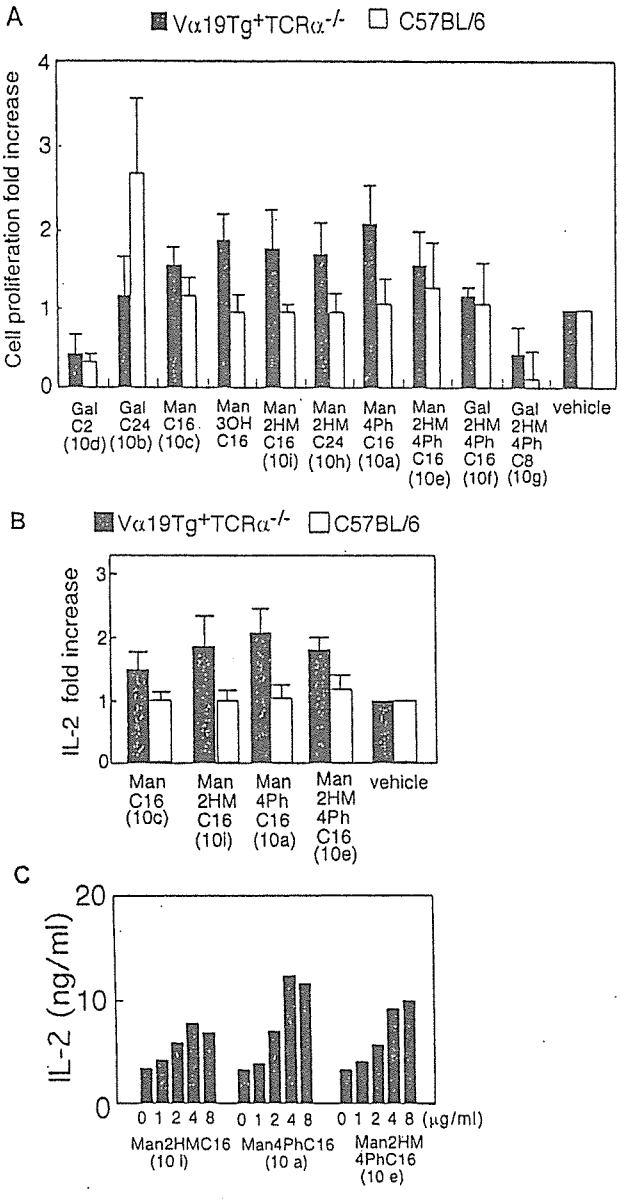

Fig. 2. Immune responses of Vα19 NKT cells in culture elicited by α-ManCer and α-GalCer derivatives. Liver MNCs from Vα19 Tg^+ $TCR\alpha^{-/-}$ and C57BL/6 mice were cultured in the presence or absence of glycolipids (2 μg ml^{-1}). After 2 days, the immune responses were monitored by measuring cell proliferation ($[^3H]$-thymidine incorporation for 5 h) (A) and IL-2 secretion in the culture fluid (B). Results are shown as the fold increase relative to the control culture with vehicle (1/200 v/v DMSO). *(C) Dose-dependent activation of Vα19 Tg^+ cells with α-ManCer derivatives. IL-2 production by Vα19 Tg^+ $TCR\alpha^{-/-}$ liver MNCs cells in the different concentration of α-ManCer derivatives was determined after 2 days of culture.*
Abbreviations of glycolipids are listed in Fig. 1.

examination of this structural modification. In contrast, a similar structural modification in the sphingosine moiety of α-GalCer decreased the antigenic activity toward Vα14 NKT cells presumably due to reduced interaction between α-GalCer and CDld.

Modified α-ManCers are possibly useful for developing new therapies for various immunological disorders, since they have potency to induce immune responses of Vα19 NKT cells not only in culture but also in vivo.

4. Experimental

4.1. General

Silica gel chromatography was performed on Merck Kiesegel 60. ^{1}H-NMR spectra were recorded on a JEOL α400 spectrometer (400 MHz, JEOL, Tokyo, Japan) using tetramethylsilane (TMS) as an internal standard. Mass spectra were

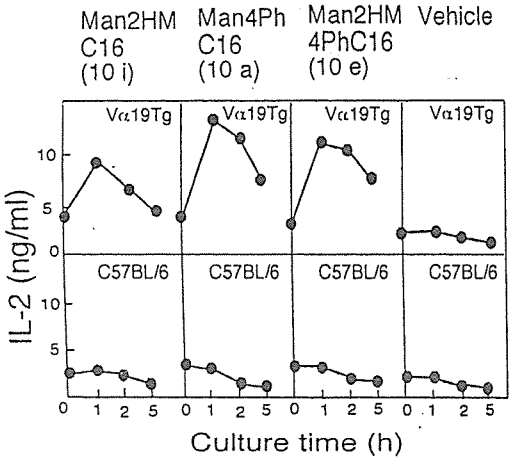

Fig. 3. Priming of Vα19 NKT cells in vivo with challenge of α-ManCer derivatives.
Spleen cells from Vα19 Tg^+ $TCR\alpha^{-/-}$ and C57BL/6 mice previously injected with glycolipids (20 μg per animal) or vehicle (DMSO) via the tail vein were cultured for the period indicated. Culture supernatants were harvested and tested for production of cytokines at the indicated time points.

measured on a JMS-DX300 (JEOL). High-resolution mass spectra were measured on a JMS700 (JEOL). Infrared spectra were recorded on an FT/IR-5300 spectrometer (JASCO, Tokyo, Japan). Elemental analyses were performed on a CHN coder MT-5 (Yanaco, Tokyo, Japan).

4.2. Synthesis of α-glycosyl ceramide analogues

4.2.1. Precursors for glycosyl acceptors

2-Amino-4-(4-octylphenyl)butanol (**1a**), 2-aminohexadecanol (**1b**) (Scheme 1), 2-amino-2-[2-(4-octylphenyl)ethyl]-1,3-propanediol (**3a**, FTY-720) and tetradeanyl-1,3-propanediol (**3b**) (Scheme 2) were obtained as described previously [10]. Optically active 2-aminohexadodecanol (*2S*-**1b**, *2R*-**1b**) were synthesized from each diastereomer of Garner's aldehyde (1, 1-dimethyl (*S*)- or (*R*)-5-formyl-2,2-dimethyl-3-oxazolidinecarboxylate) [21] as shown in Scheme 1B as previously described [22].

4.2.2. Glycosylation acceptors

The precursors were *N*-acylated with acyl chloride of an appropriate length (Schemes 1 and 2). For example, *N*-[1-hydroxymethyl-3-(4-octylphenyl) propyl] hexadecanamide (**2a**) was obtained as follows. 2-Amino-4-(4-octylphenyl) butanol (**1a**, 1.1 g, 4.0 mmol) was dissolved in pyridine (40 ml). To this solution was added chlorotrimethylsilane (1.1 ml, 8.7 mmol) in drops over 10 min at 5 °C. The solution was stirred at room temperature for 1 hour. Then palmitoyl chloride (1.4 ml, 4.6 mmol) was added in drops to the reaction solution over 10 min and the resulting mixture was stirred at the same temperature for 3 hours. After evaporation of the solvent in vacuo, the residue was dissolved in $CHCl_3$ and washed successively with water and brine, then the organic phase was separated and dried over anhydrous magnesium sulfate. After concentration, the residue was purified by recrystallization from AcOEt to give the product (**2a**) as yellow crystal (0.94 g, yield, 46%).

To prepare glycosylation acceptors for 2-amino-1,3-propanediol, one of the two hydroxymethyl groups of (**3**) was selectively *O*-bebzylated via **4** and **5**. Then, the products (**6**) were *N*-acylated to afford **7** as indicated in Scheme 2 by using standard procedures.

4.2.3. Glycosylation and removal of the protective groups

Glycosylation acceptors (**2a–d**, **7a–d**) were *O*-glycosylated with 8 (1-*O*-acetyl-2,3,4,6-tetrabenzyl-D-mannose [23], or 1-fluoro1-acetyl-2,3,4,6-tetrabenzyl-D-galactose [24]) by a Lewis acid promoter (BF_3 for 1-*O*-acetate and $SnCl_2$, $AgClO_4$ for 1-fluoride), and the adducts were subjected to hydrogenolysis to take away benzyl protective groups (Scheme 3). For instance, *N*-[1-(α-D-mannopyranosyl oxymethyl)-3-(4-octylphenyl) propyl]hexadecanamide (**10a**, *Man4PhC16*) was synthesized as follows. 1-Acetyl-2,3,4,6-tetrabenzyl-D-mannose (**2a**, 0.49 g, 0.84 mmol) was dissolved in dichloromethane (20 ml) under a nitrogen atmosphere. BF_3-OEt_2 (0.11 ml, 0.89 mmol) was added in drops over 2 min at 5 °C and the mixture was stirred for 10 min. Then a solution of **2a** (0.46 g, 0.89 mmol) in dichloromethane (7.0 ml) was added in drops over 4 min and stirred for 1.5 hours. A saturated ammonium chloride solution was added to this reaction mixture. The organic phase was *separated* and washed successively with brine and dried over anhydrous magnesium sulfate. After filtration and concentration, the residue was purified by silica gel column chromatography using a mixture of hexane: AcOEt (5:1) as an elution solvent. The yellow oil (0.47 g) of the tetrabenzyl derivative (**9a**) was dissolved in ethanol (20 ml) and stirred for 4 hours in the presence of 20% $Pd(OH)_2$ on charcoal under an hydrogen atmosphere. After filtration and concentration, the product (**10a**) was obtained as a colorless amorphous solid (0.10 g, yield, 21% from **2a**).

4.2.4. Preparation of optically active ManC16 (2S- and 2R-10c)

Diastereomers of ManC16 (2S- and **2R–10c**) were synthesized from *2S* and *2R*-diastereomers of **1b** as described for the synthesis of the racemic mixture of **10c**. The yield of the intermediate and the final products was comparable to the yield of the racemic forms *(60–70% for 2S-9c and 2R-9c)*.

4.2.5. Product data for 10a–i

4.2.5.1. 10a (Man4PhC16). Elemental analysis: calculated for $C_{40}H_{71}NO_7$ $3/2H_2O$: C; 68.14, H; 10.58, N; 1.99.

Found: C; 68.45, H; 10.64, N; 2.01.

^{1}H-NMR (CD_3OD): δ 0.87–0.90 (6H, m, methyl), 1.26 (36H, br s, methylene), 1.53–1.68 (4H, m, methylene), 2.17–2.22 (2H, m, methylene), 2.54 (2H, t, J = 7.3 Hz, methylene), 2.55–2.68 (2H, m, methylene), 3.36–3.45 (1H, m), 3.47–3.52 (1H, m), 3.55–3.61 (1H, m), 3.63–3.70 (3H, m), 3.76–3.83

(2H, m), and 3.95–4.10 (1H, m) for mannose C2, C3, C4, C5, C6a, C6b, sphingosine C1a, C1b, C2 and C3, 4.70–4.72 (1H, m, anomeric), 7.04 (2H, d, J = 8.3 Hz, phenyl), 7.07(2H, d, J = 8.3 Hz, phenyl). MS (EI), *m/z*: 677(M^+).

IR (cm^{-1}) (KBr): 3388, 2922, 2852, 2360, 1622, 1464, 1384.

Appearance: Colorless amorphous

4.2.5.2. 10b (GalC24). Elemental analysis: calculated for $C_{46}H_{91}NO_7 \cdot 3/4H2O$, C, 70.50; H, 11.90; N,1.79.

Found: C, 70.57; H, 11.91; N, 1.66.

^{1}H-NMR (CD_3OD): δ 0.80 (6H, t, 6.8 Hz, methyl), 1.19 (66H, brs, methylene), 1.45–1.60 (2H, m, methylene), 2.10 (2H, t, J = 7.3 Hz, methylene) 3.36 (1H, dd, J = 10.3, 5.4 Hz), 3.46–3.71 (6H, m), 3.77 (1H, d, J = 2.0H), and 3.90–3.94 (1H, m), for galactose C2, C3, C4, C5, C6a, C6b, sphingosine C1a, C1b, C2 and C3, 4.70 (1H, brs, anomeric).

MS (EI): *m/z*: 770 (M^+).

IR(KBr): 3433,2918,2850,1646,1543,1468.

m.p. 142–144 °C.

4.2.5.3. 10c (ManC16). Elemental analysis: Calculated for $C_{38}H_{75}NO_7 \cdot 1/2H_2O$: C,68.39; H,11.45; N,2.14.

Found: C;68.42; H,11.48; N,2.10.

^{1}H-NMR(CD_3OD): δ 0.89 (6H, t, J = 6.8 Hz, methyl), 1.28 (48H, brs, methylene), 1.59–1.67(4H, m, methylene), 2.18 (2H, t, J = 7.3 Hz, methylene), 3.38 (1H, dd, J = 9.8, 5.9 Hz), 3.46–3.52 (1H, m), 3.58 (1H, d, J = 9.3 Hz), 3.61–3.70 (3H, m), 3.78 (1H, dd, J = 3.4, 1.5 Hz), 3.81 (1H, dd, J = 11.7, 2.0 Hz), and 3.94–4.03 (1H, m), for mannose C2, C3, C4, C5, C6a, C6b, sphingosine C1a, C1b, C2 and C3, 4.72 (1H, brs, anomeric)

MS (EI): *m/z*: 658 (M^+).

m.p. 153–155 °C.

4.2.5.4. 2S-10c. Elemental analysis: Calculated for $C_{38}H_{75}NO_7 \cdot 1/2H_2O$: C, 68.42; H, 11.48; N,2.10.

Found: C; 68.39; H, 11.45; N, 2.14.

^{1}H-NMR(CD_3OD): δ 89 (6H, t, J = 6.8 Hz, methyl), 1.28 (48H, brs, methylene), 1.51–1.81 (4H, m, methylene), 2.19 (2H, t, J = 7.3 Hz, methylene), 3.41 (1H, dd, J = 9.8, 4.4 Hz), 3.46–3.53 (1H, m), 3.57 (1H, d, J = 9.8 Hz), 3.58–3.71 (3H, m), 3.78 (1H, brs), 3.82 (1H, d, J = 11.7 Hz), and 3.99–4.08 (1H, m), for mannose C2, C3, C4, C5, C6a, C6b, sphingosine C1a, C1b, C2 and C3, 4.73 (1H, brs, anomeric).

IR (KBr): 3296, 2918, 2851, 1643, 1541, 1467, 1130, 1101, 1059.

CD: $[\alpha]_D$: +19.2 (0.25, EtOH).

m.p. 147–148.

4.2.5.5. 2R-10c. Elemental analysis: Calculated for $C_{38}H_{75}NO_7 \cdot 1/2H_2O$: C, 68.42; H,11.48; N, 2.10.

Found: C; 68.39; H, 11.45; N, 2.14

NMR(CD_3OD): δ 0.89(6H, t, J = 6.8 Hz, methyl), 1.28 (48H, brs, methylene), 1.59–1.67 (4H, m, methylene), 2.18 (2H, t, J = 7.3 Hz, methylene), 3.38 (1H, dd, J = 9.8, 5.9 Hz), 3.46–3.52 (1H, m), 3.58 (1H, d, J = 9.3 Hz), 3.61–3.70 (3H, m), 3.78 (1H, dd, J = 3.4, 1.5 Hz), 3.81 (1H, dd, J = 11.7, 2.0 Hz), and 3.94–4.03 (1H, m), for mannose C2, C3, C4, C5, C6a, C6b, sphingosine C1a, C1b, C2 and C3, 4.72(1H, brs, anomeric).

IR(KBr): 3306, 2917, 2850, 1644, 1543, 1468, 1139, 1105, 1059.

Mass(EI): 658.

CD: $[\alpha]_D$ = +48.5 (0.20, EtOH).

m.p. 157–159.

4.2.5.6. 10d (GalC2). Elemental analysis: Calculated for $C_{24}H_{47}NO_7 \cdot 1/4H_2O$: C, 61.84; H, 10.27; N, 3.00.

Found: C, 61.77; H, 10.38; N, 3.07.

^{1}H-NMR (400 MHz, CD_3OD): δ 0.89 (3H, t, J = 8 Hz, methyl), 1.28 (24H, brs, methylene), 1.44–1.52 (1H, m, methylene), 1.53–1.61 (1H, m, methylene), 1.95 (3H, s, methyl), 3.33–3.37 (1H, m), 3.42–3.51 (1H, m), 3.63–3.79 (5H, m), 3.81 (1H, brs), and 3.90–4.03 (1H, m), for galactose C2, C3, C4, C5, C6a, C6b, sphingosine C1a, C1b, C2 and C3, 4.79–4.80 (1H, m, anomeric), 7.9–8.1 (1H, m, amide).

IR (cm^{-1}) (KBr): 3278, 2915, 2851, 1648, 1558, 1472.

EI-MS, *m/z*: 462 $(M + H)^+$.

4.2.5.7. 10e (Man2HM4PhC16). Elemental analysis: Calculated for $C_{41}H_{73}NO_8 \cdot H_2O$, C,67.82; H,10.41; N,1.93.

Found: C;67.55; H,10.33; N,1.91.

^{1}H-NMR (400 MHz, CD_3OD): δ 0.89(6H, t, J = 6.8 Hz, methyl), 1.27 (34H, brs, methylene), 1.53–1.65 (4H, m, methylene), 1.93–2.08 (2H, m, methylene), 2.18–2.22 (2H, m, methylene), 2.52–2.59 (4H, m, methylene), 3.52–3.57 (2H, m), 3.61–3.73 (4H, m), and 3.79–3.84 (4H, m), for mannose C2, C3, C4, C5, C6a, C6b, sphingosine C1a, C1b, C2 and C3, 4.75 (1H, d, J = 9.8 Hz, anomeric), 7.04 (2H, d, J = 7.8 Hz, phenyl), 7.08 (2H, d, J = 7.8 Hz, phenyl), 7.30 (1H, d, J = 11.2 Hz, amide).

IR (KBr): 3321, 2923, 2853, 1646, 1467.

Amorphas.

4.2.5.8. 10f (Gal2HM4PhC16). ^{1}H-NMR (400 MHz, CD_3OD): δ 0.83–0.87 (6H, m, methyl), 1.22 (34H, brs, methylene), 1.50–1.60 (4H, m, methylene), 1.90–2.08 (2H, m, methylene), 2.13–2.20 (2H, m, methylene), 2.45–2.57 (4H, m, methylene), 3.4–4.0 (10H, m), for galactose C2, C3, C4, C5, C6a, C6b, sphingosine C1a, C1b, C2 and C3, 4.78–4.85 (1H, m, anomeric), 7.00 (2H, d, J = 8 Hz, phenyl), 7.05 (2H, d, J = 8 Hz, phenyl), 7.38 (1H, d, J = 16 Hz, amide).

High resolution FAB-MS, calculated for $C_{41}H_{74}N_1O_8$ $(M + H)^+$ 708.5414; found 708.5435.

4.2.5.9. 10g (Gal2HM4PhC8). ^{1}H-NMR (400 MHz, CD_3OD): δ 0.84–0.92 (6H, m, methyl), 1.28 (18H, brs, methylene), 1.50–1.65 (4H, m, methylene), 1.90–2.10 (2H, m, methylene), 2.13–2.25 (2H, m, methylene), 2.45–2.60 (4H, m, methylene), 3.4–4.1 (10H, m), for galactose C2, C3, C4, C5, C6a, C6b, sphingosine C1a, C1b, C2 and C3, 4.78–4.85 (1H, m, anomeric), 7.04 (2H, d, J = 8 Hz, phenyl), 7.09 (2H, d, J = 8 Hz, phenyl), 7.42 (1H, d, J = 12 Hz, amide).

High resolution FAB-MS, calculated for $C_{33}H_{58}N_1O_8$ $(M + H)^+$, 596.4162; found 596.4153.